New footprints from Laetoli (Tanzania) provide evidence for marked body size variation in early hominins

Fidelis T. Masao[1], Elgidius B. Ichumbaki[1], Marco Cherin[2,3]*, Angelo Barili[4], Giovanni Boschian[5], Dawid A. Iurino[3,6], Sofia Menconero[7], Jacopo Moggi-Cecchi[8], Giorgio Manzi[9]

[1]Department of Archaeology & Heritage, College of Humanities, University of Dar es Salaam, P.O. Box 35050, Dar es Salaam, Tanzania.

[2]Dipartimento di Fisica e Geologia, Università di Perugia, Via Alessandro Pascoli, 06123 Perugia, Italy.

[3]PaleoFactory, Sapienza Università di Roma, Piazzale A. Moro 5, 00185 Roma, Italy.

[4]Galleria di Storia Naturale, Centro d'Ateneo per i Musei Scientifici, Università di Perugia, Via del Risorgimento, 06051 Deruta, Italy.

[5]Dipartimento di Biologia, Università di Pisa, Via Derna, 56126 Pisa, Italy.

[6]Dipartimento di Scienze della Terra, Sapienza Università di Roma, Piazzale A. Moro 5, 00185 Roma, Italy.

[7]Studio Associato Grassi, Via Luigi Salvatorelli 33, 06125 Perugia, Italy.

[8]Dipartimento di Biologia, Università di Firenze, Via del Proconsolo 12, 50122 Firenze, Italy.

[9]Dipartimento di Biologia Ambientale, Sapienza Università di Roma, Piazzale A. Moro 5, 00185 Roma, Italy.

***For correspondence:** marco.cherin@unipg.it

Abstract

Laetoli is a well-known palaeontological locality in northern Tanzania whose outstanding record includes the earliest hominin footprints in the world, discovered in 1978 at Site G and commonly attributed to *Australopithecus afarensis*. Here, we report hominin tracks unearthed in the new Site S at Laetoli and referred to two bipedal individuals (S1 and S2) moving on the same palaeosurface and

in the same direction as the three hominins documented at Site G. The stature estimates for S1 greatly exceed those previously reconstructed for *Au. afarensis* from both skeletal material and footprint data. Combined with a comparative reappraisal of the Site G footprints, the evidence collected here embodies very important additions to the Pliocene record of hominin behaviour and morphology. Our results are consistent with considerable body size variation and, likely, degree of sexual dimorphism within a single species of bipedal hominins as early as 3.66 million years ago.

Introduction

Estimates of body size and proportions are crucial in the evolutionary interpretation of Plio-Pleistocene hominin palaeobiology (***McHenry, 1991, 1992; Ruff et al. 1997; Grabowski et al., 2015***) and have been the subject of ongoing debates, at least since the late 1970s (e.g., ***Johanson and White, 1979***). Within-species variability in body size often relates to sexual dimorphism and/or to adaptation to different ecologies. This is particularly true among extant Hominoidea, which show diverse patterns of variation (e.g., ***Plavcan, 2001***), as for instance sexual dimorphisms in gorillas (polygynous species, with strong sexual dimorphism due to intense male-male competition) vs. chimpanzees (promiscuous, with definitively smaller sexual dimorphism). Complex relationships among body size, sexual dimorphism, mating system (and/or reproductive strategy) and social structure/behaviour reasonably apply also to extinct hominins, including our bipedal relatives of the Plio-Pleistocene. Actually, claims that size variation in *Australopithecus* and/or *Paranthropus* was larger than in recent human populations include inferences on sexual dimorphism (***Richmond and Jungers, 1995***; ***Plavcan et al., 2005***; ***Lockwood et al., 2007***; but see ***Reno et al., 2003***), while arguments referred to early *Homo* are usually associated to eco-physiological variants (***Antón et al., 2014***; ***Di Vincenzo et al., 2015***).

Regarding *Australopithecus afarensis*, a remarkable variation in size and shape within its alleged hypodigm was noted already in the original description of the species (***Johanson et al., 1978***).

Nevertheless, there have always been disputes about the nature and degree of sexual dimorphism characterising this early bipedal hominin, with supporters of either pronounced (e.g., ***Johanson and White, 1979***; ***Kimbel and White, 1988***; ***McHenry, 1991***; ***Richmond and Jungers, 1995***; ***Lockwood et al., 1996***; ***Plavcan et al., 2005***; ***Harmon, 2006***; ***Gordon et al., 2008***) or moderate (***Lovejoy et al., 1989***) body size dimorphism.

For example, ***Richmond and Jungers (1995)*** wrote: "If the fossils from Hadar and Maka (and Laetoli) are assumed […] to be from one sexually dimorphic species, then the degree of sexual dimorphism of *Au. afarensis* would have been at least as extreme as that of the most dimorphic living apes […]. It follows that a strictly monogamous structure would have been highly unlikely." ***Reno et al.*** (***2003***; but see ***Plavcan et al., 2005***, and the reply by ***Reno et al., 2005***) challenged this premise with an analysis of sexual dimorphism of femoral head diameter in *Au. afarensis*, concluding that these early hominins showed human-like sexual dimorphism and were therefore characterised by a monogamous mating system. Conversely, ***Grabowski et al.*** (***2015***, p. 90) obtained comprehensive and thoroughly vetted data, supporting "arguments that *Au. afarensis* had substantial size dimorphism […] leading to a large amount of variation in body size within this taxon."

It is clear that our ability to investigate about this important and controversial issue depends on the possibility of evaluating body size and proportions of extinct creatures. Estimates are largely inferred from known relationships between metric data in living species, such as bone length or joint size, and stature or body mass (***McHenry, 1991, 1992***; ***Grabowski et al., 2015***). Similar estimates can be even more plainly obtained from the analysis of single footprints or - even better - from trails of footprints (***Tuttle, 1987***; ***Dingwall et al., 2013***). Among these, one of the most remarkable pieces of evidence are the renowned trackways from Laetoli Site G (northern Tanzania), which are ascribed to *Au. afarensis* (***White and Suwa, 1987***).

In this paper we report about a novel set of hominin tracks discovered at Laetoli in the new Site S, comparing it to a reappraisal of the original evidence. The new tracks can be referred to two different individuals moving in the same direction and on the same palaeosurface as those documented at Site G.

The site: a brief overview

Laetoli (***Figure 1A,B***) is one of the most important palaeontological localities in Africa. It lies within the Ngorongoro Conservation Area at the southern edge of the Serengeti Plains. The region includes sites such as Olduvai Gorge, Lake Ndutu and Laetoli itself and provides a long sequence of Plio-Pleistocene mostly volcano-sedimentary deposits rich in archaeological and paleontological remains (***Hay, 1987***), overlying Precambrian metamorphic rocks. The paleoanthropological significance of the whole area is known since the mid 1930s (***Reck and Kohl-Larsen, 1936***; ***Kohl-Larsen, 1943***), whereas Laetoli became known worldwide in the 1970s for stimulating discoveries, as the holotype and other remains of *Au. afarensis* (***Leakey et al., 1976***; ***Johanson et al., 1978***) and the remarkable evidence of the earliest bipedal hominin tracks (***Leakey and Hay, 1979***; ***Leakey and Harris, 1987***) dated to 3.66 million years ago (Ma) (***Deino, 2011***).

Mammal, bird and insect prints and trails were identified in 18 sites (labelled from A to R) out of 33 total palaeontological localities in the Laetoli area (***Leakey, 1987a***; ***Harrison and Kweka, 2011***; ***Musiba et al., 2008***). Footprints occur in 10 sublevels within the so-called Footprint Tuff, corresponding to the lower part of Tuff 7 in the Upper Laetolil Beds stratigraphic sequence (***Hay, 1987***). These hominin trackways were found in 1978 at Site G (Locality 8) and were referred to three individuals (G1, G2, G3) of different body size: the smaller G1 walked side by side on the left of the larger G2, while the intermediate size G3 superimposed its feet over those of G2 (***Leakey, 1981***). The trackways are usually ascribed, not without controversy (***Tuttle et al., 1991***; ***Harcourt-Smith, 2005***), to *Au. afarensis* (***White and Suwa, 1987***), which is the only hominin taxon found to date in the Upper Laetoli Beds (***Harrison, 2011***).

Discovery and notes on preservation

The new Site S (situated within Locality 8) is located about 150 m to the south of Site G (***Figure 1C***), on the surface of the same morphological terrace. It was discovered during systematic survey and excavation activities (Cultural Heritage Impact Assessment) aimed at evaluating the impact of a proposed new field museum at Laetoli, in the area of Locality 8. Sixty-two 2x2 m-test-pits were randomly positioned within a grid and were carefully excavated down to the Footprint Tuff and sometimes deeper.

In 2015, fourteen hominin tracks always associated with tracks of other vertebrates (see Results) were unearthed in three test-pits, respectively labelled L8, M9 and TP2 from north to south (see Materials and Methods) (***Figures 1C–2***). Seven bipedal tracks in different preservation state (see below) were exposed in L8 (***Figure 2—figure supplement 1 and Figures 3–4***) and four in M9 (***Figure 2—figure supplement 2 and Figure 5***). Two additional tracks of the same individual were found in the eastern part of TP2. All these prints are clearly referable to a single individual trackway, with an estimated total length of 32 m and trending SSE-NNW (i.e., 320–330°), approximately parallel to the G1 and G2/3 trackways. Following the code used for the Site G prints (***Leakey, 1981***), we refer to the new individual as S1 (footprint numbers S1-1–7 in L8, S1-1–4 in M9 and S1-1–2 in TP2). At the end of the September 2015 field season, we discovered one more track referable to a second individual (S2), in the SW corner of TP2. Conversely, we exposed only non-hominin footprints in test-pit M10 (***Figure 2—figure supplement 3***).

The preservation state of the tracks varies considerably along the trackway, depending on the depth of the Footprint Tuff from the surface.

In L8, the Tuff is very shallow, not deeper than 20 cm to the south, whereas it even crops out on the scarp of the terrace on the opposite side. Consequently, the Tuff is overlain here only by reworked loose soil, and the tracks are not filled up with compact and/or cemented sediment. Preservation issues arise from this situation, because the tuff tends to be rather altered and dislodged along the natural fractures (***Figure 7***). The first four tracks in the L8 trail are the best preserved, whereas the state of preservation of the footprint-bearing surface is particularly critical in the northern part (***Figure 8***), where it appears very damaged by cracks of different size and by plant roots. Some parts of the surface even subsided into micro-grabens developed along the main faults. Consequently, the anterior portion of the track L8/S1-6 is no more visible because it is situated in one of these lowered parts (***Figure 3***). Moreover, a zigzag channel probably formed by a large root crosses the northern half of this test-pit from SE to NW, so that L8/S1-5 is virtually indiscernible (***Figure 3***). In the western portion of L8, three large rounded holes (green circles in ***Figure 2***) originated from roots of acacia trees that grew on the surface. Raindrop imprints are visible to the northern edge of the test-pit (***Figure 2***), on two relatively well-preserved portions of the tuff, surrounded by weathered and lowered areas. These features were already described in several other footprint-bearing sites at Laetoli (***Leakey, 1987a***).

The situation is different in M9, where about 72 cm of grey soil and unaltered sediments overlie the Footprint Tuff. Here, the tracks are sealed by the upper, laminated part of Tuff 7 and filled with strongly cemented sediment. The tuff is here in reasonably good condition, even if it is crossed by old tectonic fractures re-cemented by calcite (***Figures 5, 9***). Moreover, deeply expanding roots penetrate preferentially into the subhorizontal fissures situated between bedding planes, dislodging the rock and fostering carbonate dissolution.

The taphonomic state of the Footprint Tuff and of the tracks is very similar in M10, which is about 80 cm deep. In M9, the infilling matrix was removed from two hominin tracks (M9/S1-2 and M9/S1-3) (***Figures 5, 9***) in order to examine their inner morphology. Small amounts of water were used during the excavation, in order to soften the sediment and darken its hue to better distinguish it from the surrounding tuff. The infill was finally removed by small dental tools, trying not to damage the very thin calcite film covering the original footprint surface (***White and Suwa, 1987***). Unfortunately, some vertical crisscross fractures filled by hard calcite veins (***Figures 5, 9***) preclude a detailed morphological study of the two footprints. An about 4 cm-thick layer of tuff was removed from a footprint-free area of the M9 SW corner, putting into light a deeper horizon containing bovid tracks (***Figure 2***).

In TP2, the preservation state of the about 66 cm-deep printed tuff is intermediate between the L8 and M9/M10 ones. The southern part is in better condition: the hominin track TP2/S1-1 is rather well preserved and some of the other animal prints are still filled by the sediment of the overlying unit. Unfortunately, the SW portion of the test-pit is crossed longitudinally by north-running roots that cross TP2/S2-1, partially damaging it (***Figures 2, 6***). On the contrary, the northern part of the test-pit is poorly preserved because of a micro-graben developed along an EW-trending fault, which also crosses TP2/S1-2 causing the lowering of its anterior portion (***Figures 2, 6***).

Geological setting

The assessment of the Laetoli Site S sequence within the wider framework of the Eyasi Plateau formations is crucial to understand the stratigraphic relationships between the footprint-bearing units of the newly discovered Site S and those of the historical Site G. These relationships can be discussed at two levels of increasing detail, each one affecting different and similarly more detailed aspects of the study of the tracks.

The first - and most relevant - level regards verifying whether the unit bearing the new tracks corresponds to the Footprint Tuff, part of Tuff 7 together with the overlying Augite Biotite Tuff (***Hay, 1987***, p. 36; ***Leakey and Hay, 1979***, p. 317), where the Site G tracks were printed. This would imply that the trackways are contemporaneous from a geological/geochronometric point of view. Moreover, considering that Tuff 7 includes a sequence of several sublevels originated by distinct eruptions closely spaced in time, and that its overall deposition time was estimated in weeks (***Hay and Leakey, 1982***, p. 55; ***Hay, 1987***, p. 36), it can be concluded that all the tracks belong to the same general population of hominins.

Secondarily, stratigraphic relationships can be explored at higher detail, in order to assess whether the tracks of Site S were printed on exactly the same sublevel of the Footprint Tuff as in Site G. This aspect would concern mostly the behavioural aspects of a hypothetical single group of hominins, but it must be pointed out that extra-fine correlation between outcrops, even in a depositional environment with moderate lateral variability like the Footprint Tuff deposition area, can be affected by major uncertainty.

Field description of the sequences

The eye-scale characteristics of the profiles exposed in the test-pits are reported here from the top downwards.

Test-pit L8

The Footprint Tuff is extremely shallow and partly eroded in this area, which is limited by the erosional surface of a gully side. Only the lower subunit is preserved, whereas the upper one is completely pedogenised; consequently, the tracks are not filled-up with compact sediment, but only by modern soil, dark grey (2,5Y 4/1-4/2 *dark grey-dark greyish brown*) clay loam to sandy clay loam, with well-developed coarse subangular blocky structure, extremely loose and weak. To the north the Tuff is no longer covered by soil and crops out directly from the ground surface; the rock, already fractured by tectonic stress, is partly dislodged into decimetre-size blocklets. To the south, the Tuff is overlain by 20-25 cm of soil.

Test-pit M9 (***Figure 10***)

(1) Modern soil. Dark grey (2,5Y 4/1-4/2 *dark grey-dark greyish brown*) clay loam to sandy clay loam, with well-developed coarse subangular blocky structure, rather loose and moderately weak; sand is more common at the base, where the structure is somewhat less developed.

Few coarse unsorted skeleton. Few Fe/Mn-oxide mottles. Thickness 20-25 cm; abrupt and slightly undulating limit.

(2) Grey augite-rich tuff. Greyish (2.5Y 4/1-5/1 *dark grey-grey*) silty sand, poorly sorted, with common very coarse sand-size black rounded grains. Massive structure, moderately strong; no sedimentary structures. Thickness 32-35 cm; sharp subhorizontal limit, frequently marked by recent roots occupying a 0 to 1 cm-thick planar void. Poorly sorted very fine sand to coarse sand-size particles, including common anhedral to subhedral augite, grey rounded particles, greyish-brownish aggregates, other unidentified lithics. Light grey micro- to cryptocrystalline cement.

(3) Laminated grey tuff. Sequence of light grey to brownish to black (2.5Y 6/2 *light brownish gray*-2.5Y 5/4 *light olive brown*-N 2/5 *black*) sandy laminae and thin layers 1-3 mm-thick. Massive, very strong. Thickness 5-7 cm; sharp limit marked by a fine white crust, and in some cases by a 2-5 mm-thick planar void. Moderately well-sorted anhedral to subhedral, subrounded to subangular, medium to fine sand-size light grey to greenish grains; white microcrystalline cement. In the uppermost layers the grain-size is slightly coarser (medium sand), and the particles are subrounded to rounded; biotite laminae and brownish rounded aggregates are common. The darker laminae usually include finer grains, and the cement is generally less abundant.

(4) Finely layered grey and white tuff. Sequence of light grey to white (N6/ gray-10YR 8/1 *white*) sandy layers, 2-3 mm to 25-30 mm-thick. The uppermost level is white and thicker, even if its thickness can vary significantly throughout the surface. Platy and rounded fragments of grey sediment, probably clods deriving from disarticulation of desiccation polygons, lie horizontally within the overlying white sediment. Massive, strong. Thickness 7-8 cm; sharp subhorizontal and plain limit. Footprints at the top. The grey layers include dark grey fine sand-size particles, moderately well-sorted, rounded to subrounded, often

concentrated in mm-thick laminae at the base of the layer. Some grading is not uncommon. The cement is light grey, apparently micro- or cryptocrystalline. The grains of the white layer are somewhat larger and less sorted, subrounded to angular; medium sand-size biotite laminae are frequent, as well as very light green subhedral to anhedral crystals; brownish rounded grains occur sparsely. The cement is white, apparently micro- to cryptocrystalline.

(5) Light brown tuff. Homogeneous silty sand (7.5YR 6/3 *light yellowish brown*) with whitish mottles (10YR 7/1 *light gray*-5Y 8/1 *white*), poorly sorted and with common coarse sand-size rounded grains. Massive structure, very firm to moderately strong. Homogeneous, with traces of burrowers at the top. Base not observed. Very poorly sorted, silt to coarse sand-size particles, rounded to angular. Dominant grey rounded particles, frequent subhedral augite, few to frequent medium sand-size biotite laminae; rounded fragments of fine grey ash fall tuff and other still unidentified lithics occur sparsely. Whitish micro- to cryptocrystalline cement.

Test-pit M10

(1) Modern soil. Dark grey (2,5Y 4/1-4/2 *dark grey-dark greyish brown*) clay loam to sandy clay loam, with well-developed medium to very coarse subangular blocky structure, rather loose and moderately weak; sand is more common at the base, where the structure is somewhat less developed. Few Fe/Mn-oxide mottles. Thickness 20-45 cm; abrupt undulating limit.

(2) Grey augite-rich tuff. Greyish (2.5Y 4/1-5/1 *dark grey-grey*) silty sand, poorly sorted, with common coarse to very coarse sand-size black rounded grains. Massive structure, strong; no sedimentary structures. Thickness 25-45 cm; sharp subhorizontal limit. Poorly sorted very fine sand to coarse sand-size particles, including common anhedral to subhedral augite, grey rounded particles, greyish-brownish aggregates, other unidentified lithics.

(3) Laminated grey tuff. Finely interbedded light grey to brownish to black (2.5Y 6/2 *light brownish grey*-2.5Y 5/4 *light olive brown*-N 2/5 *black*) sandy laminae and thin layers 1-3 mm

thick. Massive, very strong. Thickness 4-6 cm; sharp limit marked by a thin planar void. Moderately well-sorted anhedral to subhedral, subrounded to subangular, medium to fine sand-size light grey to greenish grains; white microcrystalline cement. In the uppermost layers the grain-size is slightly coarser (medium sand), and the particles are subrounded to rounded; biotite laminae and brownish rounded aggregates are common. The darker laminae usually include finer grains, and the cement is generally less abundant.

(4) Finely layered grey and white tuff. Only the top surface was observed. Common animal tracks.

Test-pit TP2

(1) Modern soil. Dark grey (2,5Y 4/1-4/2 *dark grey*-*dark greyish brown*) clay loam to sandy clay loam, with well-developed fine to very coarse subangular blocky structure, loose and moderately weak. Few Fe/Mn-oxide mottles. Thickness 35-45 cm; abrupt undulating limit.

(2) Grey augite-rich tuff. Greyish (2.5Y 4/1-5/1 *dark grey-grey*) silty sand, poorly sorted, with common coarse to very coarse sand-size black rounded grains. Massive structure, strong; no sedimentary structures. Thickness 6-23 cm; sharp subhorizontal limit. Poorly sorted very fine sand to coarse sand-size particles, including common anhedral to subhedral augite, grey rounded particles, greyish-brownish aggregates, other unidentified lithics.

(3) Laminated grey tuff. Finely interbedded light grey to brownish to black (2.5Y 6/2 *light brownish grey*-2.5Y 5/4 *light olive brown*-N 2/5 *black*) sandy laminae and thin layers 1-3 mm thick. Massive, very strong. Thickness 4-5 cm; sharp limit marked by a thin planar void. Moderately well-sorted anhedral to subhedal, subrounded to subangular, medium to fine sand-size light grey to greenish grains; white microcrystalline cement. In the uppermost layers the grain-size is slightly coarser (medium sand), and the particles are subrounded to rounded; biotite laminae and brownish rounded aggregates are common. The darker laminae usually include finer grains, and the cement is generally less abundant.

(4) Finely layered grey and white tuff. Only the top surface was observed. Common animal and three hominin tracks.

Results

Non-hominin tracks

Tracks and trackways of mammals, birds and insects as well as raindrop impressions are recorded from 18 sites at Laetoli, named alphabetically from A to R. Sites from A to P were listed and geographically located by ***Leakey (1987b)***, who also described in detail the ichnological record of the most important exposures. Sites Q and R were discovered and described by ***Musiba et al. (2008)***. More than 11300 single footprints are recorded from Sites A–R. These tracks testify to a very rich ichnofauna, although a very high percentage of them (more than 88%) can be ascribed to small mammals such as lagomorphs and/or *Madoqua*-like bovids (***Leakey, 1987a***; ***Musiba et al., 2008***).

Numerous footprints were discovered in the new exposures (test-pits L8, M9, TP2, M10) of the Footprint Tuff at Site S in Locality 8 (***Figure 2***). A total of 529 footprints of mammals (excluding hominins) and birds (***Table 1***) were recorded during the September 2015 field season. The prints were carefully cleaned using soft brushes to reveal detailed features, measured, photographed, traced, mapped and identified in a preliminary study.

Mammal tracks - mostly of small and medium-size bovids - are very abundant in M10, L8 and M9 and occur less frequently in TP2. Their size (30–40 mm long and 20–36 mm wide) and morphological features suggest that most of them can be ascribed to the genus *Madoqua* (***Figure 2 and Figure 2—figure supplement 3***). Some slightly larger prints (60–80x40–60 mm) can be referred to medium-sized bovids such as *Gazella*, *Eudorcas* or *Nanger*.

It is very difficult to distinguish the footprints of *Madoqua*-like bovids from the lagomorph ones because of the very similar morphology and size (***Leakey, 1987a***). Consequently, we decided to ascribe to Lagomorpha only trails clearly including at least four footprints, arranged in the normal hare gait pattern, i.e. two single prints left by the front feet followed by a couple of prints made by the hind feet in the direction of gait. Each single trail (i.e., four footprints) is approximately 200 mm long and 100 mm in wide.

We identified very few prints of giraffids in M10 (about 170x125 mm), equids in L8 and M9 (about 50–95x45–70 mm) and rhinoceroses in M9 (about 150–135 mm) (***Figure 2 and Figure 2—figure supplement 3C***). In M9 and M10, some avian prints (about 60x75 mm) often organized in trails, can be referred to Galliformes of the family Numididae, such as the guinea fowl (genus *Numida*) (***Figure 2 and Figure 2—figure supplement 3A,B***). Finally, we report some very small (about 10x10 mm) tracks of unidentified animals, probably micromammals in M9 and M10.

The above-mentioned assemblage of terrestrial mammal and bird footprints suggests that the local palaeoenvironment was characterized by a mosaic of dry tropical bushland, woodland, open grassland and riverine forest similar to extant one.

Morphology of hominin tracks

The morphology of the S1 tracks can be described in detail, while unfortunately the only preserved track of S2 shows an abnormal widening of the anterior part. This enlarged morphology is possibly due to a lateral slipping of the foot before the toe-off, or to taphonomic factors, since a thick root crossing the footprint longitudinally may have altered its original morphology. The overall morphology of the S1 tracks matches those at Site G (***Figure 11***) and is similar in particular to the prints of the larger individual G2 (***Robbins, 1987***): the heel has an oval shape and is pressed deeply into the ground; the medial side of the arch is higher than the lateral one; the ball region is oriented at an angle of about 75° with respect to the longitudinal axis of the foot and is delimited anteriorly by a transversal ridge, formed when the toes gripped the wet ash and pushed it posteriorly. No clear distinction among the toes is visible. The adducted hallux extends more anteriorly than the other toes in all visible footprints. In TP2/S1-1 the hallux apparently shuffled anteriorly when the foot was lifted from the ground. Some tracks (especially L8/S1-3, M9/S1-2, M9/S1-3 and TP2/S1-1) are characterised by a posterior drag mark about 100-mm long (***Figures 4–7 and Figure 2—figure supplements 1 and 2***). This was possibly left by the heel shuffling on the ash before being firmly placed into the soil. The two latter features were recognised also in some of the G2 prints (***Robbins, 1987***) and suggest that the feet were probably lifted above the ground with a low oblique angle. The depth distribution pattern indicates that the weight transfer of S1 was similar to what was described for G1–3 (***Robbins, 1987***): starting from the heel, the weight was transferred along the lateral part of the foot (note the steep slope of the lateral wall of the tracks compared to that on the medial side) up to the distal metatarsal region, and from here to the toes. However, in some of the S1 tracks (L8/S1-1, L8/S1-3 and TP2/S1-8, all of the right side), the area of maximum depth is located beneath toes 2–5. This may suggest a somewhat asymmetrical walking, in which the weight was sometimes loaded on the anterolateral part of the foot before the toe-off. Alternatively, this pattern may be indicative of a rotation of the upper body during the gait (***Schmid, 2004***). The angle of gait ranges approximately from 2° to 11°, without any particular difference between the right and left sides. Regarding this aspect, S1 resembles more G2/3, for which very low average angles are reported, whereas G1 shows instead wider and asymmetrical angles (***Tuttle, 1987***).

Speed, stature and body mass estimates

The main dimensional parameters of the tracks at Site S are presented in ***Table 2*** (the single measurements are explained in Materials and Methods)

Speed estimates for S1 and G1–3 were computed starting from stride length (***Figure 3***) (see Materials and Methods). The obtained values (***Table 3***) show that these hominins were all walking at similar low speed (about 0.44 to 0.9 m/s, depending on the analysis method).

The average length of the tracks in the S1 trackway is 261 mm (range 245–274). Lower values were measured for the three individuals at Site G. The average lengths are 180 mm for G1, 225 mm for G2 and 209 mm for G3 (***Leakey, 1981***; ***Tuttle, 1987***) (***Table 3***), although a digital analysis-based study (***Bennett et al., 2016***) of some Site G footprint casts suggests higher values for G1 (193 mm) and G3 (228 mm). The main metrical features of the S1 and S2 tracks (footprint length and width, step and stride lengths) are larger than the G1–3 equivalents (***Table 3***).

The stature and mass of the Laetoli print-makers were estimated following the relationships between foot/footprint size and body dimensions (***Tuttle, 1987***; ***Dingwall et al., 2013***). It must be pointed out that stature and body mass estimates obtained by linear regressions from modern humans (***Tuttle, 1987***; first method by ***Dingwall et al., 2013***) are probably exaggerations, since the body proportions of modern *H. sapiens* are considerably different from those of the Laetoli putative track-makers. Consequently, we focused our interpretations on the more appropriate predictions inferred from the relationship between foot size and body dimensions in *Australopithecus* (second method by ***Dingwall et al., 2013***; see Materials and Methods for details). The data in ***Tables 2–3*** indicate that stature and mass estimates for S1 and S2 (about 165 cm and 44.7 kg, and 146 cm and 39.5 kg respectively) are higher than those obtained for G1, G2 and G3 (with S2 partly overlapping the higher estimates for G2).

Discussion

Stratigraphic position of the new tracks

Site S is situated on an almost level or very gently dipping surface, situated at the foot of the left (southern) side of the Garusi River valley. Site G is situated about 150 m to the north, on the same surface but 1.5-2 m lower than Site S. Several shallow gullies dissect this surface, originating a complexly terraced morphology: consequently, there is no observable stratigraphic continuity between the two sites. However, the gullies put into light about 2-3 m of the underlying sequence, whose units are horizontally layered and characterised by almost constant thickness. Only a shallow depression elongated E-W can be observed between the sites, probably an ancient erosion channel filled by a constant thickness of the Site S footprint-bearing tuff. Even if the area of possible outcrop of the Footprint Tuff on gully sides close to Site S is covered by debris, the correlation between G and S is in general straightforward.

All previous literature describing the original stratigraphic setting at Laetoli (***Leakey, 1979***; ***Hay and Leakey, 1982***; ***Hay, 1987***) indicates that the Footprint Tuff can be divided into two main units - the lower and the upper one - which can be subdivided into respectively 14 and 4 sublevels. Footprints occur on several sublevels of each unit all over the Laetoli area: eight within the lower one (mostly on sublevel 9 and on the topmost sublevel 14), and two within the upper one (sublevels 1 and 2).

Leakey and Hay (***1979***, pp. 317–318 and fig. 4) provided a brief description of the type-sequence of the Footprint Tuff at Locality 6 (site A), where a short trackway of human-like footprints - later referred to an ursid (***Tuttle, 2008***) - was also found. Later on, ***Hay and Leakey*** (***1982***, p. 55) and ***White and Suwa*** (***1987***, p. 488) specified that the hominin tracks at Site G are situated on the top of horizon B, i.e. the top of sublevel 14 within the lower unit of the Footprint Tuff. Eventually, ***Hay*** (***1987***, pp. 34–35 and fig. 2.6) provided a generalized columnar profile of the Footprint Tuff, which is by far the most accurate description available, but is averaged over all the Laetoli area sites. Although the above stratigraphic descriptions are very accurate, they do not provide details about the eye-scale characteristics of the tuffs, i.e. colour, texture, limits, etc., nor photographs of the sequence are published.

The Site S sequence is not fitting perfectly the aforementioned descriptions, at least within the observed area, which is rather narrow. The grey augite-rich tuff of Site S largely matches the description of the Augite Biotite Tuff described by ***Hay*** (***1987***, p. 34 and following, level 4 in fig.

2.6, p. 35). Regarding the Footprint Tuff, the upper unit corresponds to Site S Laminated Grey Tuff, but the sublevels are here layered rather crudely, whereas the most evident sedimentary structure is a very fine and almost continuous lamination, which makes the subdivision rather problematic. Energy-sorting of denser grains is apparently a relevant aspect of the depositional processes. The Finely Layered Grey and White Tuff of Site S corresponds to the lower subunit of the Footprint Tuff; the sublevels are apparently 14 as in the standard description, but the number may be imprecise - or evaluated differently - because some of them are extremely thin and apparently discontinuous; in fact, some of the thinner (and darker) ones look more like concentrations of gravity-sorted coarser/denser grains situated at the bottom of graded layers. The top sublevel is rather thicker than the other ones and somewhat whitish instead of greyish, as apparently also in Localities 6 and 7.

Some lateral variability is not surprising in continental environments, which are normally affected by strong morphogenetic processes and/or lateral changes in the sedimentary environments. Consequently, lateral variability can be expected also within the sequence of the Footprint Tuff, even if the involved volcanic depositional processes were rather uniform over a wide area around Laetoli and gave the whole sequence a remarkably homogeneous aspect throughout its outcrops.

The correlation between Site G and Site S cannot be absolutely undisputable, at least for the time being, because the original profile could not be examined directly. However, the geological and morphological setting of the area, as well as the characteristics of the newly exposed sequence, indicate with a very good margin of confidence that the newly discovered tracks belong to the Footprint Tuff.

Regarding a more accurate correlation within the Footprint Tuff, it can be observed that the Site S tracks were printed on the uppermost level of the Finely Layered Grey and White Tuff (unit 4 in the description provided in this paper), which corresponds to the lower subunit of the Footprint Tuff. The lithological change to the overlying subunit is very evident and marked by a sharp surface, often underlined by a thin crack. However, because of the aforementioned dissimilarities, it cannot be assessed with reasonable confidence whether this stratigraphic position also corresponds to the top of level 14 in the standard sequence (***Hay, 1987***, p. 35, fig. 2.6), i.e. to the same stratigraphic position as the Site G trackways.

Implications of the new Laetoli footprints

Our results show that no matter which method is employed to estimate stature and body mass (see Material & Methods), the two individuals S1 and S2 were taller and had a larger body mass than the G individuals. The estimated about 165 cm stature of S1 is quite remarkable, exceeding G2 by more than 20 cm (***Table 3***).

In order to contextualise the australopithecine and early *Homo* stature estimates and range of variability obtained from the footprints into a broader picture (***Figure 12***), and to compare them with a larger sample, we extended our analysis to consistent data based on skeletal elements, namely femurs (see Materials and Methods for details). ***Figure 12*** shows the estimated stature of australopithecine and early *Homo* individuals by species between 4.0 and 1.0 Ma. The predicted stature of S1 exceeds any australopithecine: a mean value of 158 cm was estimated for the large *Au. afarensis* individual from Woranso-Mille (***Haile-Selassie et al., 2010***; ***Lovejoy et al., 2016***), while the Hadar individuals range from 109 to 143 cm (***McHenry, 1991***; ***Ward et al., 2012***) (***Figure 12***). The stature of S1 falls within the range of modern *Homo sapiens* maximum values; it also fits the available *Homo erectus sensu lato* estimates based on fossil remains (***Ruff and Walker, 1993***) and on footprints (***Bennett et al., 2009***) (***Figure 12***). At the same time, the 41 to 48 kg body mass range estimated for S1 (***Table 3***) falls easily within the range of male *Au. afarensis* (40.2–61.0 kg) (***Grabowski et al., 2015***). These results extend the dimensional range of the Laetoli track-makers and identify S1 as a large-size individual, probably a male (***Plavcan, 1994***; ***Grabowski et al., 2015***).

This in turn provides independent evidence for large body size individuals among hominins as ancient as 3.66 Ma. Consequently, we may emphasise the conclusions by ***Grabowski et al. (2015)*** and ***Jungers et al. (2016),*** i.e. that the body size of the australopithecines and of the early *Homo* representatives was similar, but also that certain australopithecine individuals (at least of *Au. afarensis*) were comparable with later *Homo* species, including *H. erectus s. l.* and *H. sapiens*. Thus, our results support a nonlinear evolutionary trend in hominin body size (***Di Vincenzo et al., 2015; Jungers et al., 2016***) and contrast with the idea that the emergence of the genus *Homo* and/or the first dispersal out of Africa was related to an abrupt increase in body size (***McHenry and Coffing, 2000***; ***Antón et al., 2014***; ***Maslin et al., 2015***). The identification of large-size individuals among the australopithecines - i.e. hominins commonly presumed to be small-bodied on average - shows also that the available fossil record can be misleading, resulting in an underestimate of the hominin phenotypic diversity in any given period.

Moreover, ascribing the S1 tracks to a possible male requires reconsidering sex and age of the other Laetoli individuals, who have been object of a plethora of interpretations (and associated illustrations largely disseminated to the public) since Mary Leakey's work (***Leakey, 1981***). The most parsimonious option is that sex and age of the hominins represented at Site G cannot be determined, as subadult individuals can possibly be present among them. However, the body mass estimates suggest some observations, since G1 and G3 fall within the range of putative *Au. afarensis* females (25.5–38.1 kg, according to ***Grabowski et al., 2015***), whereas G2 and S2 span across the upper female and the lower male (40.2–61.0 kg, according to ***Grabowski et al., 2015***) ranges. All these individuals are definitively smaller than the body mass resulting from the S1 tracks. A possible tentative conclusion is that the various individual represented at Laetoli respectively are: S1, a male; G2 and S2, females; G1 and G3, smaller females or juvenile individuals.

Evidence for either marked or moderate body size variation in *Au. afarensis*, based on data collected in a single site, was limited until now to the fossil assemblage from Hadar 333 locality, dated to 3.2 Ma (with body masses ranging from 24.5 to 63.6 kg). The new estimates resulting from the Laetoli individuals indicate an even more marked body size variation within the same hominin population, at 3.66 Ma. Consequently, the combined records from Laetoli and Hadar suggest that large-bodied hominins existed in the African Pliocene for over 400.000 years, between 3.66 and 3.2 Ma. At the same time, these data are in contrast with the hypothesis of a temporal trend of body size increase among *Au. afarensis* between the more ancient Laetoli and the more recent Hadar fossil samples (***Lockwood et al., 2000***).

The impressive record of bipedal tracks from Laetoli Locality 8 (Site G and the new Site S) may open a window on the behaviour of a group of such remote human ancestors, envisaging a scenario with at least five individuals (G1, G2, G3, S1 and S2) walking in the same time frame, in the same direction and at a similar moderate speed. This aspect must be evaluated in association with the pronounced body size variation within the sample, which implies marked differences between age ranges and a considerable degree of sexual dimorphism in *Au. afarensis*. Significant implications about the social structure of this stem hominin species derive from these physical and behavioural characteristics, suggesting that reproductive strategies and social structure among at least some of the early bipedal hominins we know so far were closer to a gorilla-like model than to chimpanzees or modern humans.

Eventually, the discovery reported here opens up the intriguing possibility that additional hominin trails may also occur in the area between Site G and Site S.

Materials and Methods

Geology

Extended geological observations were carried out in the Laetoli area, mostly in the nearby historical Localities 6 and 7 (***Leakey, 1987b***), in order to compare the sequences exposed there with the new Site S sequence and assess its stratigraphic position. Unfortunately, the correlation with the stratigraphic sequence of Site G (Locality 8) is impossible because this historical site is completely covered by protection features and cannot be used for direct comparison.

In Site S, field observation and detailed sequence descriptions were carried out on excavation profiles following the standard formalized by ***Catt (1990)***.

Basic observations on grain size, shape and mineralogy were carried out in the field by 10x magnification hand lens. Higher detail analyses were carried out in laboratory, under a standard Leica stereomicroscope.

Excavation and footprint imaging

The survey of the new tracks at Site S in September 2015 was focused on obtaining 3D models for documentation and morphometric analysis. The survey method is the *Structure from Motion* technique, an image-based process supported by *in situ* topographic measurements. This technique was chosen because of its technical advantages (relatively short time of data acquisition and processing; light and handy equipment; reduced costs), compared to excellent results in terms of resolution.

The equipment used in the fieldwork is a DSLR camera with 15.3 (4853 x 3198) megapixels and two different lenses: EF 24 mm f/2.8 for general shots of the excavations and EF 50 mm f/1.4 USM for details of the tracks. When necessary, the camera was mounted on a 4 m-long telescopic rod. A measuring tape and a water level were used for the measurement of the control points (i.e., circular targets with 35 mm diameter). Considering the small size of the surfaces to be detected, this measuring technique provided very high accuracy results.

Fieldwork

Hominin and non-hominin tracks were recognised in four test-pits at Site S, namely L8, M9, TP2 and M10. The original 2x2 m square shape of L8 - the first test-pit where bipedal tracks were discovered - was modified *in itinere* in order to follow the trail and consequently took the complex shape in ***Figure 2*** (southern side: 2 m; western oblique side: 4 m). M9 was excavated some 14 m to the SSE of L8 and kept the planned size of 2x2 m. Following the interpolated alignment of the bipedal trackway, a third smaller test-pit, TP2 (1x1.2 m) (***Figure 6***) was excavated at some 8 m to the SSE of M9. Finally, a fourth test-pit, M9 (2x3 m) was excavated about 15 m to the east of M9 (***Figure 2***).

After the excavation, the 52 targets of the control point system were immediately positioned: 14 in L8, 10 in M9, 14 in TP2 and 14 in M10. Each test-pit was entirely surveyed at lower resolution and then detailed 3D models of some inner portions (single prints or groups of close prints) were acquired (***Figures 4–6***). We positioned 4 perimeter targets on the ground at the corners of each test-pit, and 4 inner targets around each sub-area surveyed in detail. The following list shows the target IDs in relation to the 4 test-pits and selected areas (AF: animal footprints):

- L8. Perimeter control points: A-B-C-D; footprint L8/S1-1: target 1-2-3-4; footprint L8/S1-2: target 3-4-5-6; footprint L8/S1-3: target 5-6-7-8; footprint L8/S1-4: target 7-8-9-10.
- M9. Perimeter control points: E-F-G-H; footprint M9/S1-2: target 21-22-23-24; footprint M9/S1-3: target 23-24-25-26.
- TP2. Perimeter control points: I-J-K-L; footprint TP2/S2-1: target 27-28-29-30; footprint TP2/S1-1: target 31-32-33-34; footprint TP2/S1-2: target 33-34-35-36.
- M10. Perimeter control points: M-N-O-P; AF1: target 11-12-13-14; AF2: target 13-15-19-20; AF3: target 15-16-17-18.

In order to optimize the timing of the fieldwork, we decided not to model in detail some of the hominin tracks, i.e. L8/S1-5 (visible only in its posterior portion) L8/S1-6 (virtually invisible due to the poor state of preservation of the Footprint Tuff), L8/S1-7 (damaged and excessively deep due to the lowering of the tuff cropping out on the scarp of the terrace), M9/S1-1 and M9/S1-4 (both filled by compact matrix).

In the second step, the perimeter target positions were measured. We placed two rods equipped with spherical level on successive pairs of targets and we marked points at the same height on the rods for each pair by using the water level device. The vertical distance between these points and the targets, as well as their mutual distance were recorded. Repeating this process for all pairs of targets, the relative plan position and the height of the control points were determined respectively by trilateration and by levelling.

A preliminary accuracy check was carried out during fieldwork, by using trilateration graphic rules in plan, and by the method of successive levelling for heights. By assigning a z-coordinate to the first control point, all subsequent coordinates were derived from addition and subtraction of heights between two successive points. The check was performed by computing the algebraic sum of all height differences, and by verifying that the obtained value was close to zero. Finally, the error obtained in each test-pit was distributed to every z-coordinate of the points, in order to reduce it (***Supplementary file 1***).

The photographic survey was carried out by three shooting modes: (I) using the camera with the 24-mm lens, mounted on a telescopic rod at 4 m above the test-pits, in order to record each test-pit, as well as the spatial connection between test-pits; (II) using the camera freehand with the 24-mm lens, in order to acquire additional shots of each test-pit; (III) using the camera close to the ground with the 50-mm lens, in order to acquire detailed sub-areas. More than 2000 photos were taken, for a total of about 50 GB.

Data processing

Data processing started by checking measurements in plan and height. This step is preliminary to the definition of the control point coordinates. The trilateration method was used to obtain xy coordinates of the control points in plan. For each test-pit, six measurements were taken at the same height: the length of the four sides of the perimeter and the length of the two diagonals. Redundant measurements were used to compute the errors. In addition to a preliminary graphical control by CAD software (Autodesk AutoCAD), the automatic calculation software MicroSurvey STAR*NET was used to adjusts rigorously by least squares technique a new set of xy coordinates and heights of the control points (***Supplementary file 2***). The report provided by the software shows that the residues of adjustments never exceeded 10 mm (***Supplementary file 2***), which are a fully acceptable figure considering the size of the test-pits.

Once the adjusted xyz coordinate of all the control points (***Supplementary file 3***) were computed, we used them to scale and locate in the 3D space the 3D models built by the *Structure from Motion* technique (see below).

The pictures were first calibrated to reduce lens geometric distortion, and tone adjustment was applied in order to homogenize them and reduce the effects of different lighting condition during shooting. Subsequently, the software Agisoft Photoscan was used to generate 3D spatial data starting from the pictures, through the following phases: (I) alignment of the images; (II) creation of the *dense point cloud*; (III) transformation of the dense point cloud into a surface (*mesh*); (IV) application of the texture to the mesh (***Supplementary file 4***). A series of orthophotos (with and without textures) were extracted from the 3D models (***Figure 2—figure supplement 1, 2 and 3 and Figure 11—figure supplement 1***). A check on dense point cloud density was also carried out by CloudCompare, software for 3D point cloud and triangular mesh processing (***Figure 2—figure supplement 1, 2 and 3 and Figure 11—figure supplement 1***).

Digital survey of the cast of the G1 and G2/3 trails

At the end of the September 2015 field season, we also surveyed a first generation fiberglass cast of the southern portion of the Site G trackway (about 4.7 m in length) (***Figure 11***), kept at the Leakey Camp at Olduvai Gorge. The cast includes the following tracks in the direction of walking: G1-39, 38, 37, 36, 35, 34, 33, 27, 26, 25 on the western side and G2/3-31, 30, 29, 28, 27, 26, 25, 24, 20, 19 and 18 on the eastern side. Data acquisition and processing (***Supplementary file 4***) were performed following the same workflow described above for the Site S test-pits. We positioned

4 perimeter control points and 11 inner targets. The latter were used to model in detail six selected tracks (G2/3-29, G1-35, G1-34, G2/3-26, G2/3-25 and G2/3-18, listed in the direction of walking) (***Figure 11—figure supplement 1***).

Morphometric analysis

Morphometric data acquisition

The 3D data obtained by the above-explained procedures were also used in the morphometric analysis of the hominin tracks by Golden Software Surfer software. This contouring and surface modelling software transforms xyz data into maps (***Figures 4–6 and 11***). The xyz-format files were imported into the software and transformed into grid files. The software uses randomly spaced xyz data to create regularly spaced grids composed of nodes with xyz coordinates. The *triangulation with linear interpolation* gridding method was applied, because it works best with data that are evenly distributed over the grid area. This method uses data points to create a network of triangles without edge intersections and computes new values along the edges. It is fast and does not extrapolate beyond the z-value of the data range; in addition, it assigns blanking values to grid nodes located outside the data limits. The grid spacing was set on 1 mm.

The following morphometric measures were taken on the contour maps:

- Footprint length: maximum distance between the anterior tip of the hallux and the posterior tip of the heel;
- Footprint max width: width across the distal metatarsal region;
- Footprint heel width;
- Angle of gait: angle between the midline of the trackway and the longitudinal axis of the foot;
- Step length: distance between the posterior tip of the heel in two successive tracks;
- Stride length: distance between the posterior tip of the heel in two successive tracks on the same side.

All the above measurements were also taken manually both on the original tracks during the September 2015 field season, and on 1:1 scale sketches of the test-pits, hand-drawn on transparent plastic sheets. Morphometric values in ***Table 2*** are averaged from the results provided by the three above methods in order to reduce errors. A synthesis of data extracted from ***Table 2*** is reported in ***Table 3***. The foot index is defined as the percentage ratio between the max width and length of footprints.

Morphometric data of the G1 and G2/3 trails

Seventy human-like tracks arranged in two parallel trails (39 prints in G1 and 31 in G2/3) are reported at Laetoli Site G (***Leakey, 1981***). Unfortunately, the whole set of morphometric data of the unearthed tracks was never published, but only average values obtained from a selected number of them were provided. In the case of G2/3, data are incomplete largely because the prints of G3 are superimposed to those of G2, so that it is difficult to collect the measurements (***Tuttle, 1987***). According to ***Leakey (1981)***, only two (unspecified) prints of G2 are measurable. Morphometric data about the Site G bipedal trails are summarized in ***Table 3***, compared to the equivalent measurements taken on S1 and S2. Footprint length and maximum width for G1 and G3 are from ***Tuttle (1987)*** (average values obtained from 9 and 8 prints, respectively). Similar values are reported by ***Leakey (1981)***, while slightly higher length values were recently published (***Bennett et al., 2016***) based on digital analysis of footprints casts (G1: 193 mm, N=11; G3: 228 mm, N=5). The length of G2 footprints (225 mm) is averaged from the two values of 210 and 240 mm reported for the only two measurable prints of G2 ***(Leakey, 1981)***. Similarly, the footprint max width of G2 (117 mm) is taken from ***Leakey (1981)*** (unknown sample size for this average). The average step and stride lengths for G1 and G3 are from ***Tuttle (1987)***, while those for G2 are from ***Robbins (1987)***.

Stature, body mass and speed estimates

We used the footprint size to estimate the stature of the Laetoli track-makers by means of different approaches. The easiest method follows ***Tuttle (1987)*** and consists in estimating the stature starting from the footprint length, considering the ratio between foot length and stature in modern humans. Given that the foot length in *H. sapiens* is generally about 14 to 16% of stature (***Tuttle, 1987*** and references therein), we computed two estimates for the Laetoli hominins assuming that their feet were respectively 14 and 16% of their body height (***Tables 2–3***). This method, however, is not fully reliable because it is based on body proportions of modern humans, and because it does not take into account that the footprint length does not accurately reflect the foot length. For this last reason, we also estimated the stature using the method of ***Dingwall et al. (2013)***, who published some equations based on regressions of stature by footprint length in modern Daasanach people (Lake Turkana area, Kenya). In particular, given the probable low walking speed of the Laetoli hominins (see below), we used the "walk only" equation (Standard Error of Estimate, SEE = 5.4) (***Dingwall et al., 2013***). Indeed, the obtained results (***Tables 2–3***) fall within the range of statures estimated with the first method (except for G1 and G3, for which slightly higher statures were calculated). Finally, to assess how the results were influenced by considering modern human data, we also computed some estimates using the foot:stature ratio known for *Au. afarensis* (***Dingwall et al., 2013***). Since this ratio is 0.155–0.162 (***Dingwall et al., 2013***), we obtained stature estimates (***Tables 2–3***) predictably close to or slightly lower than the lower limit of the estimates given by the ***Tuttle (1987)*** method.

Similarly, we estimated the body mass of the Laetoli track-makers using the "walk only" regression equation that relates footprint area (i.e., footprint length x max width) and body mass (SEE = 3.7) (***Dingwall et al., 2013***). In S2 only, we used the relationship between the footprint length and body mass (SEE = 3.8) (***Dingwall et al., 2013***) because of the enlarged morphology of TP2/S2-1. As for the stature, we re-calculated the mass using the known ratio between foot length and body mass in *Au. afarensis* (0.543–0.632) (***Dingwall et al., 2013*** and references therein). The latter method resulted in estimates significantly lower than those computed by the aforementioned regression equation based on modern human data (***Tables 2–3***).

In both the described methods, mean estimates of stature and body mass for S1 were computed by averaging the estimates obtained from individual tracks (***Tables 2–3***). The average footprint length values were considered more reliable than minimum values (which from a theoretical point of view could be regarded as more representative of the foot length) for the following reasons:

(1) Previous studies demonstrated that footprint length can overestimate (***White and Suwa, 1987***) but also underestimate (***Dingwall et al., 2013***) the actual foot length. Consequently, the average footprint length can be considered as the most reliable parameter for the estimation of body dimensions (***White, 1980***; ***Tuttle, 1987***; ***Tuttle et al., 1990***; ***Dingwall et al., 2013***; ***Avanzini et al., 2008***; ***Bennett et al, 2009***; ***Roberts, 2009***).

(2) In the specific case of the S1 trackway, the length of the three smaller tracks (***Table 2***) is likely underestimated: in L8/S1-1 (length: 250 mm) the anterior edge is poorly preserved and M9/S1-1 and M9/S1-4 (length: 245 mm) are still filled of sediment (see Introduction).

It must be pointed out that the stature and body mass estimates for S2 must be considered with caution being based on a single preserved footprint. The same goes for G2, given the very low number of tracks for which the length can be measured (***Leakey, 1981***).

We also drew some inferences about the walking speed (***Table 3***), which is closely related to the stride length: in two individuals of the same body size, the one walking faster shows longer stride length. Nevertheless, the body proportions (i.e., stature, h) of the track-maker must be considered, because they influence the stride length (L) and consequently velocity (v). We followed the power law computed by ***Alexander (1976)***

$$v = 0.25g^{0.5}L^{1.67}h^{-1.17} \quad (1)$$

where g is the gravitational acceleration (9.81 m/s^2). The equation (1) is widely used to estimate walking speed in humans and other animals (**Bennett and Morse, 2014** and references therein).

Speed was further estimated following the method of ***Dingwall et al. (2013)***. We used the regression equation that relates the speed and the ratio between stride length and average footprint length for each trail, obtaining values (***Table 3***) about twice those calculated with the equation (1). The transitional speed from walk to run is around 2.2 m/s (***Dingwall et al., 2013***). As the speed of the Laetoli track-makers is significantly lower than 2.2 m/s, we used the "walk only" regression equation (***Dingwall et al., 2013***) for our speed estimates.

After computing the walking speed of S1 and G1–3 with the aforementioned two methods, we obtained the relative speed (i.e., walking speed/estimated stature) (***Table 3***), which is a good indicator to compare the gait of different individuals regardless of their body proportions.

Stature estimate comparisons

Figure 12 was designed in order to graphically compare the stature estimates of the Laetoli individuals with those obtained for other hominin specimens. With the exception of the other footprint locality taken into account, Ileret in Kenya (***Bennett et al., 2009***; ***Dingwall et al., 2013***), all other stature data are based on skeletal elements, namely femurs.

Early hominin stature reconstructions are notoriously not easy to assess: the limited number of intact long bones available in the fossil record often requires to first reconstruct the long bone length from fragmentary remains, then to use different methods to estimate the stature; eventually, the results can differ according to the method employed. Thus, in an attempt to provide a synthetic picture of stature among australopithecines and early *Homo* and to ensure that the results are comparable, we relied on a limited number of different datasets. Data are presented in ***Supplementary file 5***.

For the geological age of the considered specimens and for their taxonomic attributions we followed ***Grabowski et al. (2015)***, unless otherwise indicated.

Two kinds of femur lengths were used for stature reconstruction: (a) femur length of intact bones or femur length estimates based on reconstructions of incomplete bones; (b) femur length estimates based on femur head diameters (FHD), according to the method given in ***McHenry (1991)***. Morphometric data about complete or reconstructed femurs derive from ***McHenry (1991)***, unless otherwise indicated (mostly fossils discovered after 1991). FHD values are from ***Grabowski et al. (2015)***.

The two different equations cited in ***McHenry (1991)*** and in ***Jungers et al. (2016)*** were employed in stature reconstructions. As put into evidence in ***Supplementary file 5***, results are largely equivalent, with minor differences not relevant for the purpose of this analysis. Consequently, we used ***Jungers et al. (2016)*** stature estimates to compile ***Figure 12***.

Access to material

Three-dimensional data are available from the MorphoSource digital repository (http://morphosource.org).

Acknowledgments

This research is supported by the Italian School of Palaeoanthropology (University of Perugia; www.paleoantropologia.it), under the auspices of the Italian Ministry of Foreign Affairs and International Cooperation (*Italian archaeological, anthropological and ethnological missions abroad*) and the Italian Embassy in Dar es Salaam, Tanzania. The authors are grateful to the museum project consultant P. Rich and to the Ngorongoro Conservation Area Authority, without whom this discovery would have never been made; D. M. Kamamba, Director of Antiquities; B. B. Mapunda and Y. Kangalawe for setting-up the survey and for financial support; E. Kazimoto for preliminary geological analysis; R. Rettori for the organization of the field season; S. Grassi and A. Grassi for

3D data processing and logistical support, R. Pellizzon for photographs; P. Blasi, M. Lombardi, G. Peter, L. Quattrini, B. Zamagni, A. Songita and his assistants for the field work. R. Blumenschine, M. Haeusler, O. Kullmer, J. Njau, Y. Rak, B. Wood and R. Wunderlich provided useful comments on an earlier version of the paper.

Additional files

Supplementary files

- Supplementary file 1. Footprint imaging, measurement report 1.
- Supplementary file 2. Footprint imaging, measurement report 2.
- Supplementary file 3. Footprint imaging, measurement report 3.
- Supplementary file 4. Footprint imaging, measurement report 4.
- Supplementary file 5. Individual fossil ages, localities and estimated statures used to build ***Figure 12***.

References

Alexander RMN. 1976. Estimates of speeds of dinosaurs. *Nature* **261**:129–130. doi: 10.1038/261129a0.

Antón S, Potts R, Aiello LC. 2014. Evolution of early *Homo*: an integrated biological perspective. *Science* **345**. doi: 10.1126/science.1236828.

Avanzini M, Mietto P, Panarello A, De Angelis M, Rolandi G. 2008. The Devil's Trails: Middle Pleistocene human footprints preserved in a volcanoclastic deposit of southern Italy. *Ichnos* **15**:179–189. doi: 10.1080/10420940802470458.

Bennett MR, Harris JW, Richmond BG, Braun DR, Mbua E, Kiura P, Olago D, Kibunjia M, Omuombo C, Behrensmeyer AK, Huddart D, Gonzalez S. 2009. Early hominin foot morphology based on 1.5-million-year-old footprints from Ileret, Kenya. *Science* **323**:1197–1201. doi: 10.1126/science.1168132.

Bennett MR, Morse SA. 2014. *Human footprints: fossilised locomotion?* New York: Springer.

Bennett MR, Reynolds SC, Morse SA, Budka M. 2016. Laetoli's lost tracks: 3D generated mean shape and missing footprints. *Scientific Reports* **6**:21916. doi: 10.1038/srep21916.

Catt JA. 1990. Paleopedology manual, *Quaternary International* **6**:1–95. doi: 10.1016/1040-6182(90)90002-L.

Cole TM, Smith FH, 1987. An odontometric assessment of variability in *Australopithecus afarensis*. *Human Evolution* **2**:221–234. doi: 10.1007/BF03016108.

Deino AL. 2011. ^{40}Ar/^{39}Ar dating of Laetoli, Tanzania. In: Harrison T, editor. *Paleontology and Geology of Laetoli: Human Evolution in Context, Vol. 1.* New York: Springer. p77–97.

Di Vincenzo F, Rodriguez L, Carretero JM, Collina C, Geraads D, Piperno M, Manzi G. 2015. The massive fossil humerus from the Oldowan horizon of Gombore I, Melka Kunture (Ethiopia, >1.39 Ma). *Quaternary Science Rev*iews **122**:207–221. doi: 10.1016/j.quascirev.2015.05.014.

Dingwall HL, Hatala KG, Wunderlich RE, Richmond BG. 2013. Hominin stature, body mass, and walking speed estimates based on 1.5 million-year-old fossil footprints at Ileret, Kenya. *Journal of Human Evol*ution **64**:556–568. doi: 10.1016/j.jhevol.2013.02.004.

Gordon AD, Green DJ, Richmond BG. 2008. Strong postcranial size dimorphism in *Australopithecus afarensis*: results from two new resampling methods for multivariate data sets with missing data. *American Journal of Physical Anthropology* **135**:311–328. doi: 10.1002/ajpa.20745.

Grabowski M, Hatala KG, Jungers WL, Richmond BG. 2015. Body mass estimates of hominin fossils and the evolution of human body size. *Journal of Human Evolution* **85**:75–93. doi: 10.1016/j.jhevol.2015.05.005.

Haile-Selassie Y, Latimer BM, Mulugeta A, Deino AL, Gibert L, Melilo SM, Saylor BZ, Scott GR, Lovejoy CO. 2010. An early *Australopithecus* post-cranium from Woranso-Mille, Ethiopia. *PNAS* **107**:12121–12126. doi: 10.1073/pnas.1004527107.

Harcourt-Smith WEH. 2005. Did *Australopithecus afarensis* make the Laetoli footprint trail? New insights into an old problem. *American Journal of Physical Anthropology* **S40**:116. doi: 10.1002/ajpa.20217.

Harmon EH. 2006. Size and shape variation in *Australopithecus afarensis* proximal femora. *Journal of Human Evolution* **51**:217–227. doi: 10.1016/j.jhevol.2006.01.009.

Harrison T. 2011. Hominins from the Upper Laetolil and Upper Ndolanya Beds, Laetoli. In: Harrison T, editor. *Paleontology and Geology of Laetoli: Human Evolution in Context, Vol. 2*. New York: Springer. p141–188.

Harrison T, Kweka A. 2011. Paleontological localities on the Eyasi Plateau, including Laetoli. In: Harrison T, editor. *Paleontology and Geology of Laetoli: Human Evolution in Context, Vol. 1*. New York: Springer. p17–45.

Hay RL. 1987. Geology of the Laetoli area. In: Leakey MD, Harris JM, editors. *Laetoli: A Pliocene site in northern Tanzania.* Oxford: Clarendon. p23–47.

Hay RL, Leakey MD. 1982. The fossil footprints of Laetoli. *Scientific American* **246**:50–57.

Johanson DC, White TD. 1979. A systematic assessment of early African hominids. *Science* **202**:312–330. doi: 10.1126/science.104384.

Johanson DC, White TD, Coppens Y. 1978. A new species of the genus *Australopithecus* (Primates: Hominidae) from the Pliocene of eastern Africa. *Kirtlandia* **28**:1–14.

Jungers WL, Grabowski M, Hatala KG, Richmond BG. 2016. The evolution of body size and shape in the human career. *Philosophical Transactions of the Royal Society B* **371**:20150247. doi: 10.1098/rstb.2015.0247.

Kimbel WH, White TD. 1988. Variation, sexual dimorphism and the taxonomy of *Australopithecus*. In: Grine FE, editor. *Evolutionary history of the "robust" australopithecines*. New York: Aldine de Gruyter. p. 175–192.

Kohl-Larsen L. 1943. *Auf den Sporen des Vormenschen*. Stuttgart: Strecker und Schröder.

Leakey MD. 1981. Tracks and tools. *Philosophical Transactions of the Royal Society B* **292**:95–102.

Leakey MD. 1987a. Animal prints and trails. In: Leakey MD, Harris JM, editors. *Laetoli: A Pliocene site in northern Tanzania.* Oxford: Clarendon. p451–489.

Leakey MD. 1987b. Introduction. In: Leakey MD, Harris JM, editors. *Laetoli: A Pliocene site in northern Tanzania.* Oxford: Clarendon. p1–22.

Leakey MD, Harris JM. 1987. *Laetoli: A Pliocene site in northern Tanzania*. Oxford: Clarendon.

Leakey MD, Hay RL. 1979. Pliocene footprints in the Laetolil Beds at Laetoli, northern Tanzania. *Nature* **278**:317–323. doi:10.1038/278317a0.

Leakey MD, Hay RL, Curtis GH, Drake RE, Jackes MK, White TD. 1976. Fossil hominids from the Laetoli Beds. *Nature* **262**:460–466. doi: 10.1038/262460a0.

Lockwood CA, Kimbel WH, Johanson DC. 2000. Temporal trends and metric variation in the mandibles and dentition of *Australopithecus afarensis*. *Journal of Human Evolution* **39**:23–55. doi: 10.1006/jhev.2000.0401.

Lockwood CA, Menter CG, Moggi-Cecchi J, Keyser AW. 2007. Extended male growth in a fossil hominin species. *Science* **30**:1443–1446. doi: 10.1126/science.1149211.

Lockwood CA, Richmond BG, Jungers WL, Kimbel WH. 1996. Randomization procedures and sexual dimorphism in *Australopithecus afarensis*. *Journal of Human Evolution* **31**:537–548. doi: 10.1002/ajpa.21183.

Lovejoy CO, Kern KF, Simpson SW, Meindl RS. 1989. A new method for estimation of skeletal dimorphism in fossil samples with an application to *Australopithecus afarensis*. In: Giacobini G, editor. *Hominidae: Proceedings of the 2nd International Congress of Human Paleontology*. Milano: Jaka Book. p.103–108.

Lovejoy CO, Latimer BM, Spurlock L, Haile-Selassie Y. 2016. Chapter 8: The pelvic girdle and limb bones of KSD-VP-1/1. In: Haile-Selassie Y, Su DF, editors. *The postcranial anatomy of* Australopithecus afarensis*: New insights from KSD-VP-1/1*. Dordrecht: Springer. p.155–178.

Maslin MA, Shultz S, Trauth MH. 2015. A synthesis of the theories and concepts of early human evolution. *Philosophical Transactions of the Royal Society B* **370**:20140064. doi: 10.1098/rstb.2014.0064.

McHenry HM. 1988. New estimates of body weight in early hominids and their significance to encephalization and megadontia in robust australopithecines. In: Grine FE, editor. *Evolutionary history of the "robust" australopithecines*. New York: Aldine de Gruyter. p. 133–148.

McHenry HM. 1991. Femoral length and stature in Plio-Pleistocene hominids. *American Journal of Physical Anthropology* **85**:149–158. doi: 10.1002/ajpa.1330850204.

McHenry HM. 1992. Body size and proportions in early hominids. *American Journal of Physical Anthropology* **87**:407–431. doi: 10.1002/ajpa.1330870404.

McHenry HM, Coffing K. 2000. *Australopithecus* to *Homo*: transformations in body and mind. *Annual Review of Anthropology* **29**:125–146. doi: 10.1146/annurev.anthro.29.1.125.

Musiba CM, Mabula A, Selvaggio M, Magori CC. 2008. Pliocene animal trackways at Laetoli: research and conservation potential. *Ichnos* **15**:166–178. doi: 10.1080/10420940802470383.

Plavcan JM. 1994. Comparison of four simple methods for estimating sexual dimorphism in fossils. *American Journal of Physical Anthropology* **94**:465–476. doi: 10.1002/ajpa.1330940403.

Plavcan JM. 2001. Sexual dimorphism in primate evolution. *Yearbook of Physical Anthropology* **44**:25–53.

Plavcan JM, Lockwood CA, Kimbel WH, Lague MR, Harmon EH. 2005. Sexual dimorphism in *Australopithecus afarensis* revisited: How strong is the case for a human-like pattern of dimorphism? *Journal of Human Evolution* **48**:313–320. doi: 10.1016/j.jhevol.2004.09.006.

Reck H, Kohl-Larsen L. 1936. Erster Überblick über die jungdiluvialen Tier- und Menschenfunde Dr. Kohl-Larsen's im nordöstlichen Teil des Njarasa-Grabens (Ostafrika) und die geologischen Verhältnisse des Fundgebietes. *Geologische Rundschau* **27**:401–441.

Reno PL, Meindl RS, McCollum MA, Lovejoy CO. 2003. Sexual dimorphism in *Australopithecus afarensis* was similar to that of modern humans. *PNAS* **100**:9404–9409. doi: 10.1073/pnas.1133180100.

Reno PL, Meindl RS, McCollum MA, Lovejoy CO. 2005. The case is unchanged and remains robust: *Australopithecus afarensis* exhibits only moderate skeletal dimorphism. A reply to Plavcan et al. *Journal of Human Evolution* **49**:279–288. doi: 10.1016/j.jhevol.2005.04.008.

Richmond BG, Jungers WL. 1995. Size variation and sexual dimorphism in *Australopithecus afarensis* and living hominoids. *Journal of Human Evolution* **29**:229–245. doi: 10.1006/jhev.1995.1058.

Robbins LM. 1987. Hominid footprints from Site G. In: Leakey MD, Harris JM, editors. *Laetoli: A Pliocene site in northern Tanzania.* Oxford: Clarendon. p497–502.

Roberts G. 2009. Ephemeral, subfossil mammalian, avian and hominid footprints within Flandrian sediment exposures at Formby Point, Sefton Coast, north west England. *Ichnos* **16**:33–48. doi: 10.1080/10420940802470730.

Ruff CB, Trinkaus E, Holliday TW. 1997. Body mass and encephalization in Pleistocene *Homo*. *Nature* **387**:173–176. doi: 10.1038/387173a0.

Ruff CB, Walker A. 1993. Body size and body shape. In: Walker AC, Leakey REF, editors. *The Nariokotome* Homo erectus *Skeleton*. Cambridge: Harvard University Press. p234–265.

Schmid P. 2004. Functional interpretation of the Laetoli footprints. In: Meldrum DJ, Hilton CE, editors. *From biped to strider: the emergence of modem human walking, running, and resource transport*. New York: Springer. p49–62.

Susman RL, Stern JT, Jungers WL. 1984. Arboreality and bipedality in the Hadar hominids. *Folia primatologica* **43**:113–156.

Tuttle RH. 1987. Kinesiological inferences and evolutionary implications from Laetoli bipedal trails G-1, G-2/3, and A. In: Leakey MD, Harris JM, editors. *Laetoli: A Pliocene site in northern Tanzania.* Oxford: Clarendon. p503–522.

Tuttle RH. 2008. Footprint clues in hominid evolution and forensics: lessons and limitations. *Ichnos* **15**:158–165. doi: 10.1080/10420940802467892.

Tuttle RH, Webb DM, Baksh M. 1991. Laetoli toes and *Australopithecus afarensis*. *Human Evolution* **6**:193–200.

Tuttle RH, Webb D, Weidl E, Baksh M. 1990. Further progress on the Laetoli trails. *Journal of Archaeological Science* **17**, 347–362. doi: 10.1016/0305-4403(90)90028-4.

Ward CV, Kimbel WH, Harmon EH, Johanson DC. 2012. New postcranial fossils of *Australopithecus afarensis* from Hadar, Ethiopia (1990 – 2007). *Journal of Human Evolution* **63**:1–51. doi: 10.1016/j.jhevol.2011. 11.012.

White TD. 1980. Evolutionary implications of Pliocene hominid footprints. *Science* **208**:175–176. doi: 10.1126/science.208.4440.175.

White TD, Suwa G. 1987. Hominid footprints at Laetoli: facts and interpretations. *American Journal of Physical Anthropology* **72**:485–514. doi: 10.1002/ajpa.1330720409.

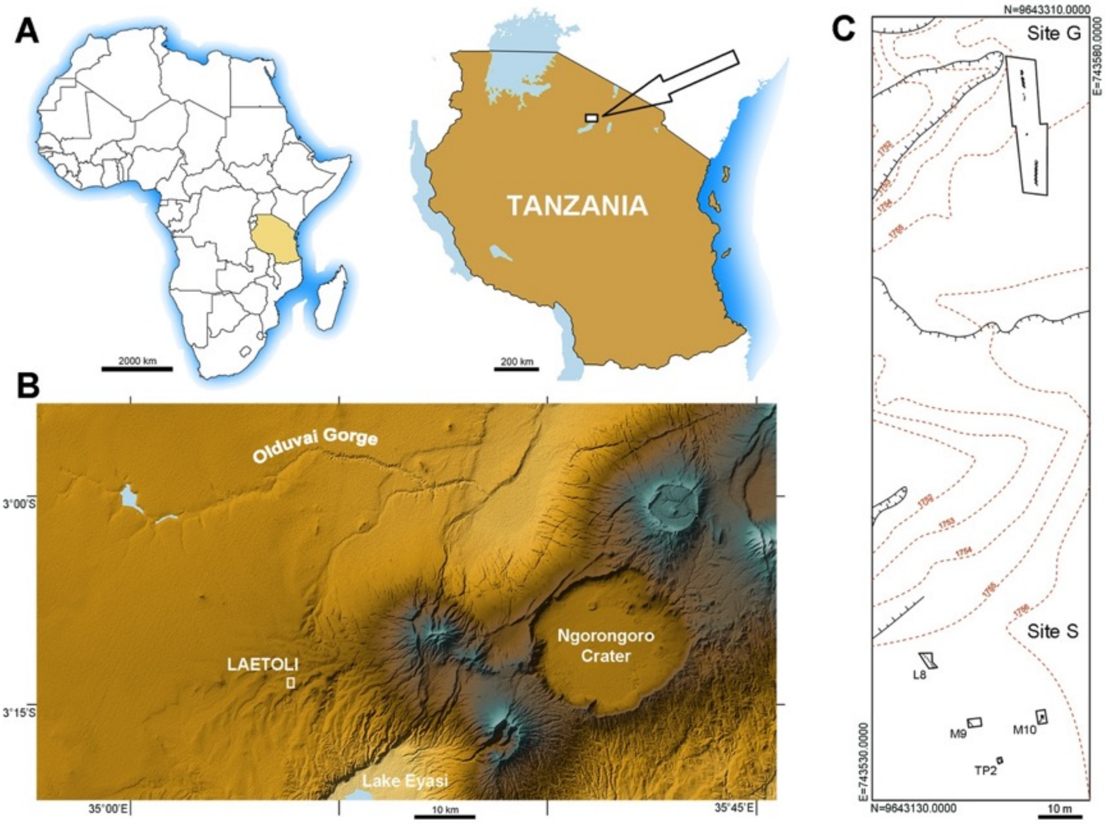

Figure 1. Geographical location and site map. (**A**) Location of the study area in northern Tanzania. (**B**) Location of Laetoli within the Ngorongoro Conservation Area, about 50 km south of Olduvai Gorge. (**C**) Plan view of the area of Laetoli Locality 8 (Sites G and S).

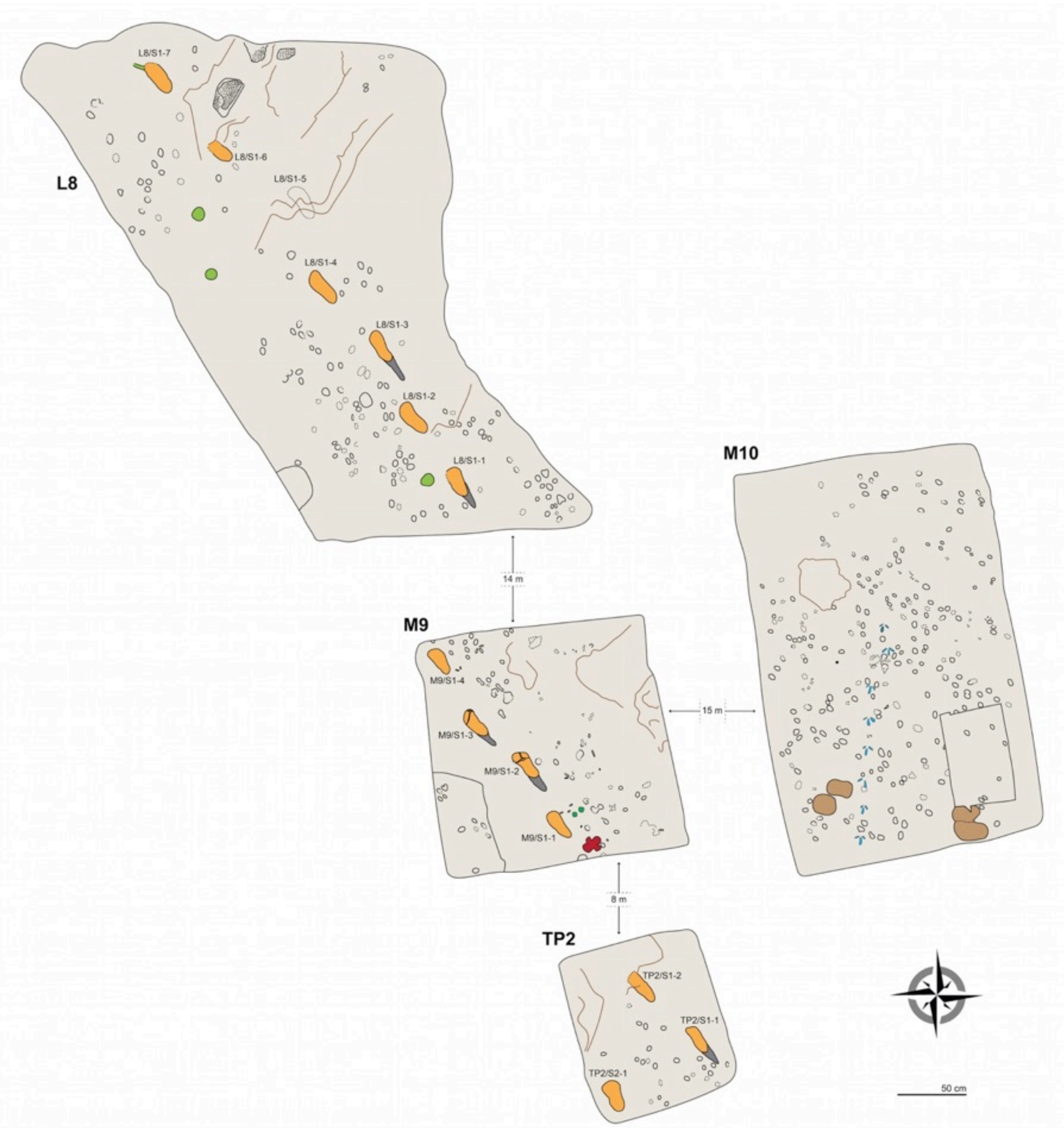

Figure 2. Plan view of the four test-pits excavated at Laetoli Site S. Dashed lines indicate uncertain contours. Some of the most interesting tracks are coloured: hominins in orange (heel drags in dark grey), equid in dark green (M9), rhinoceros in red (M9), giraffe in light brown (M10), guineafowl in blue (M10). Large roots and bases of trees are in light green (L8). The main faults/fractures are indicated by brown lines. Raindrop impressions occur in the northern part of L8 (dotted areas).

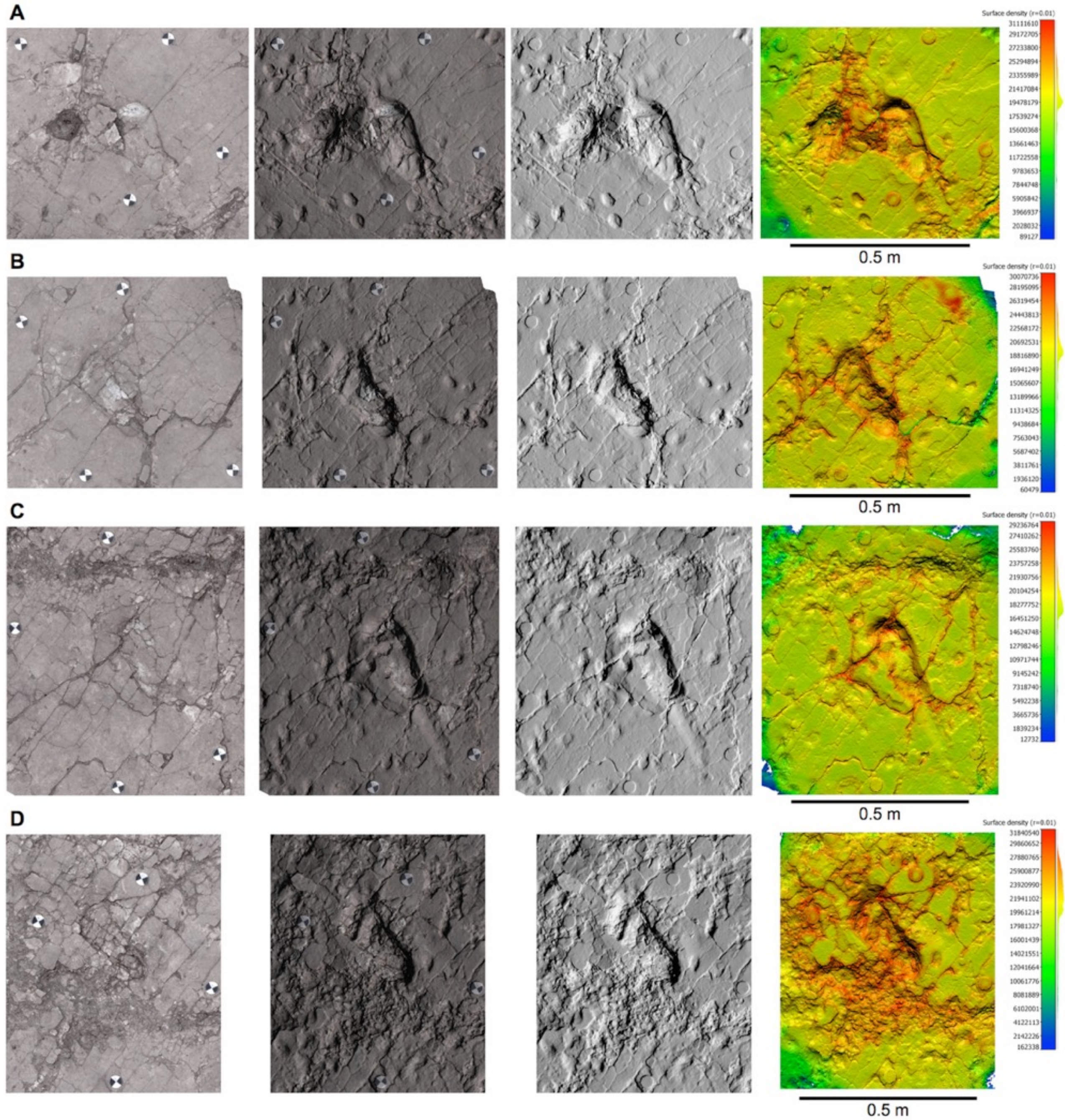

Figure 2—figure supplement 1. Orthophotos of selected hominin tracks from test-pit L8 at Site S. (**A**) L8/S1-1. (**B**) L8/S1-2. (**C**) L8/S1-3. (**D**) L8/S1-4. From left to right: textured models, textured and shaded models, shaded models, and shaded coloured models. Colours represent the density of the point clouds by determining the distance to the nearest neighbour. The surface density is the number of neighbours divided by the neighbourhood surface = $N/(\pi R^2)$.

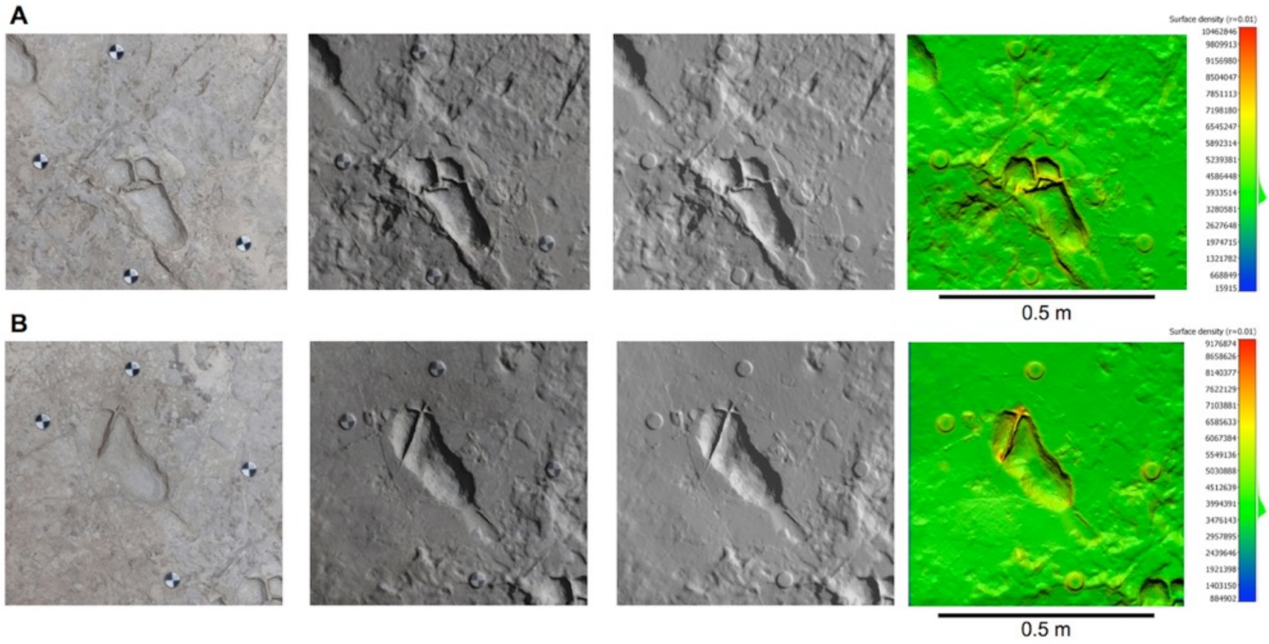

Figure 2—figure supplement 2. Orthophotos of selected hominin tracks from test-pit M9 at Site S. (**A**) M9/S1-2. (**B**) M9/S1-3. Details as in **Figure 2—figure supplement 1**.

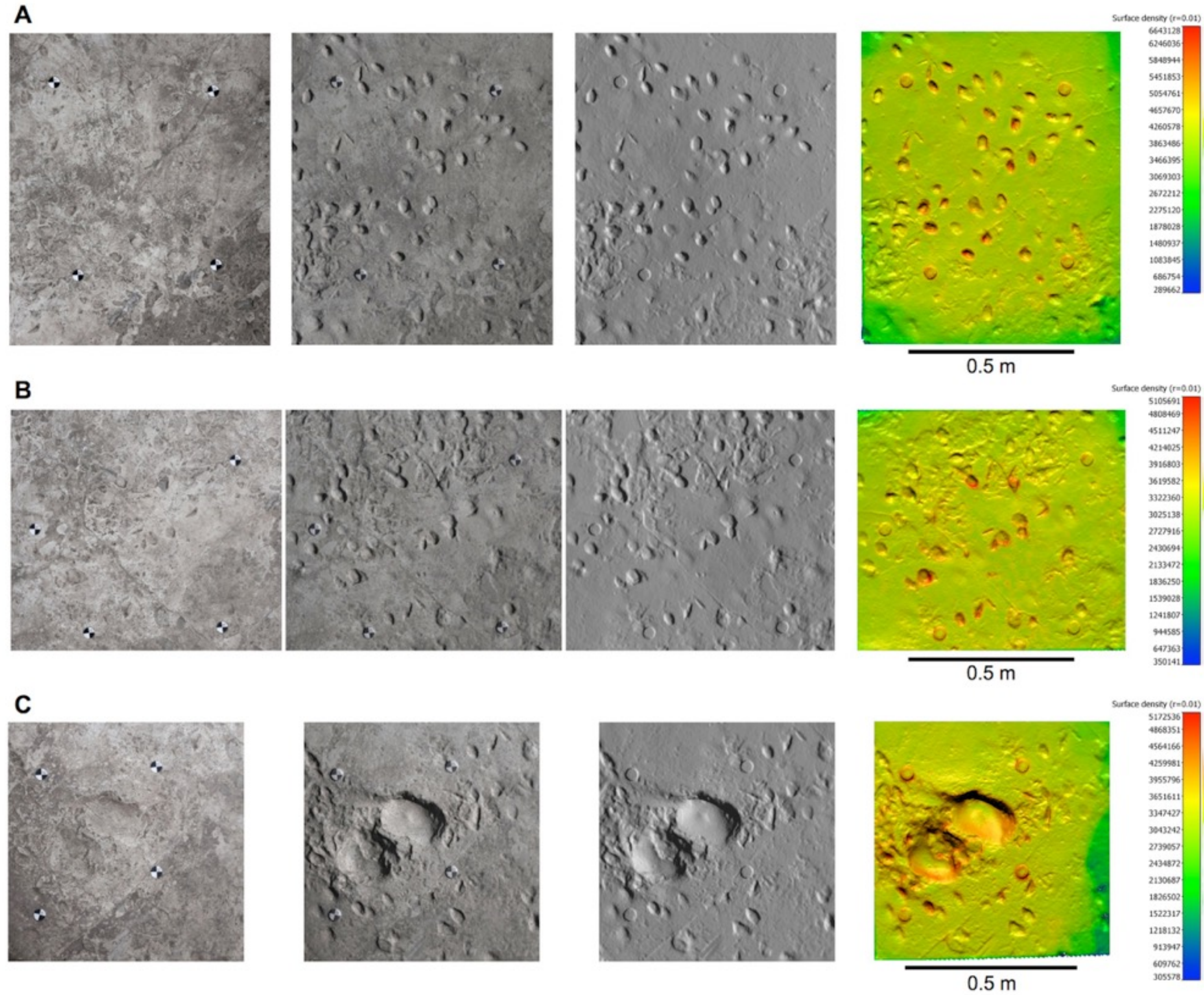

Figure 2—figure supplement 3. Orthophotos of selected hominin tracks from test-pit M10 at Site S. (**A,B**) Small bovid (?*Madoqua*) and bird (?*Numida*) tracks. (**C**) Two giraffe tracks surrounded by small bovid and bird tracks. Details as in **Figure 2—figure supplement 1**.

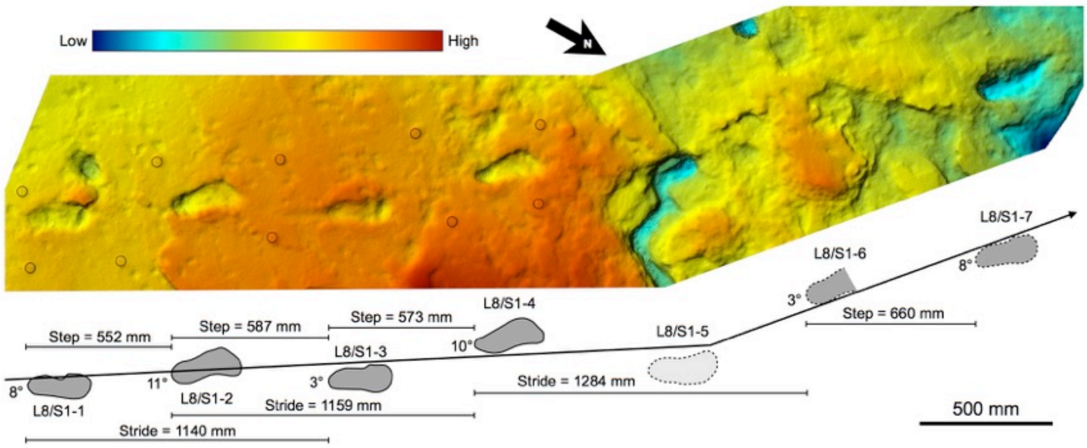

Figure 3. Shaded 3D photogrammetric elevation model of the L8 trackway. Colour renders heights as in the colour bar. The empty circles indicate the position of the targets of the 3D imaging control point system (see Materials and Methods for details).

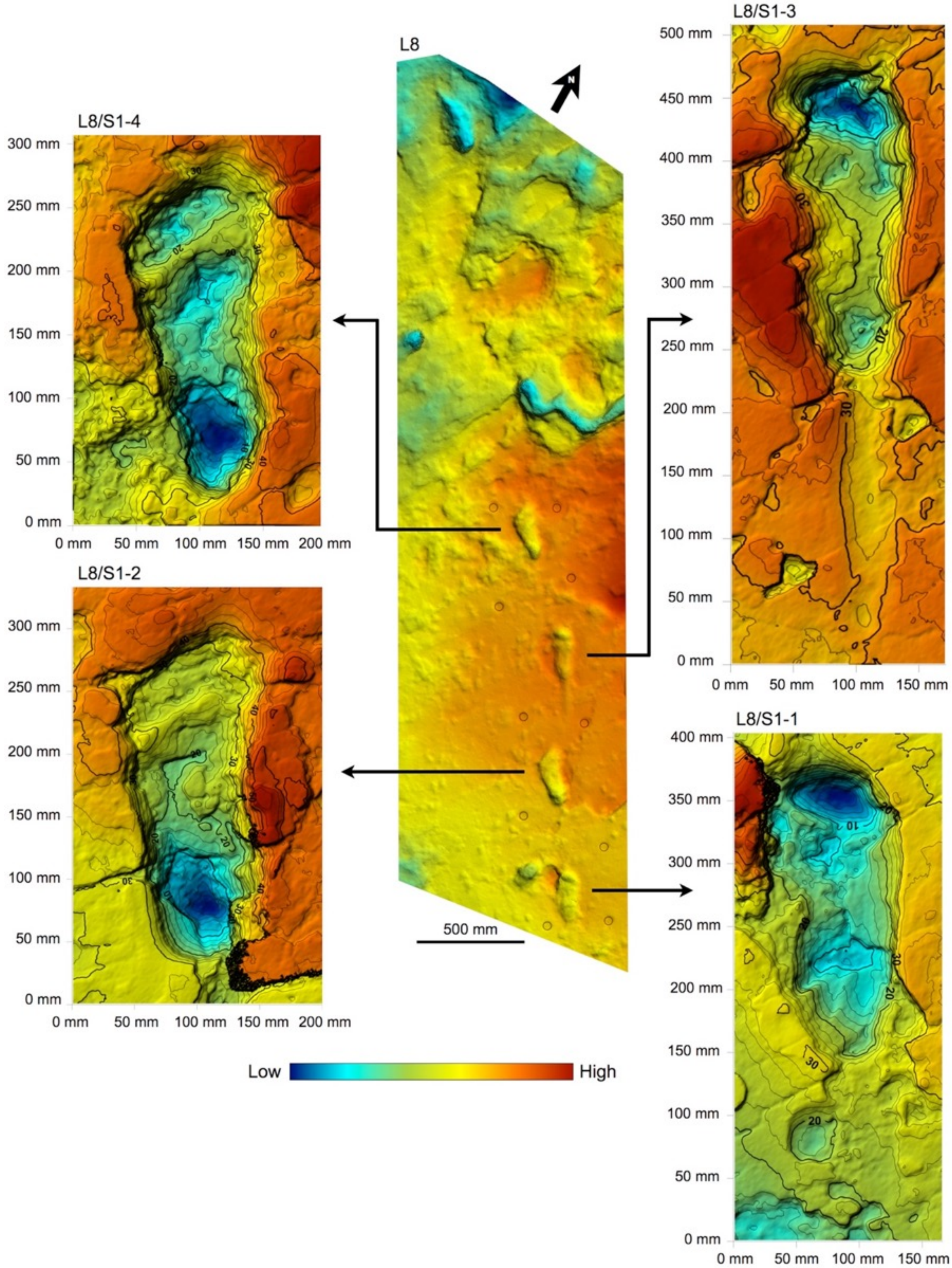

Figure 4. Shaded 3D photogrammetric elevation model of test-pit L8 and close-up of the best-preserved tracks with contour lines. Colour renders heights as in the colour bar; distance between elevation contour lines is 2 mm. The empty circles indicate the position of the targets.

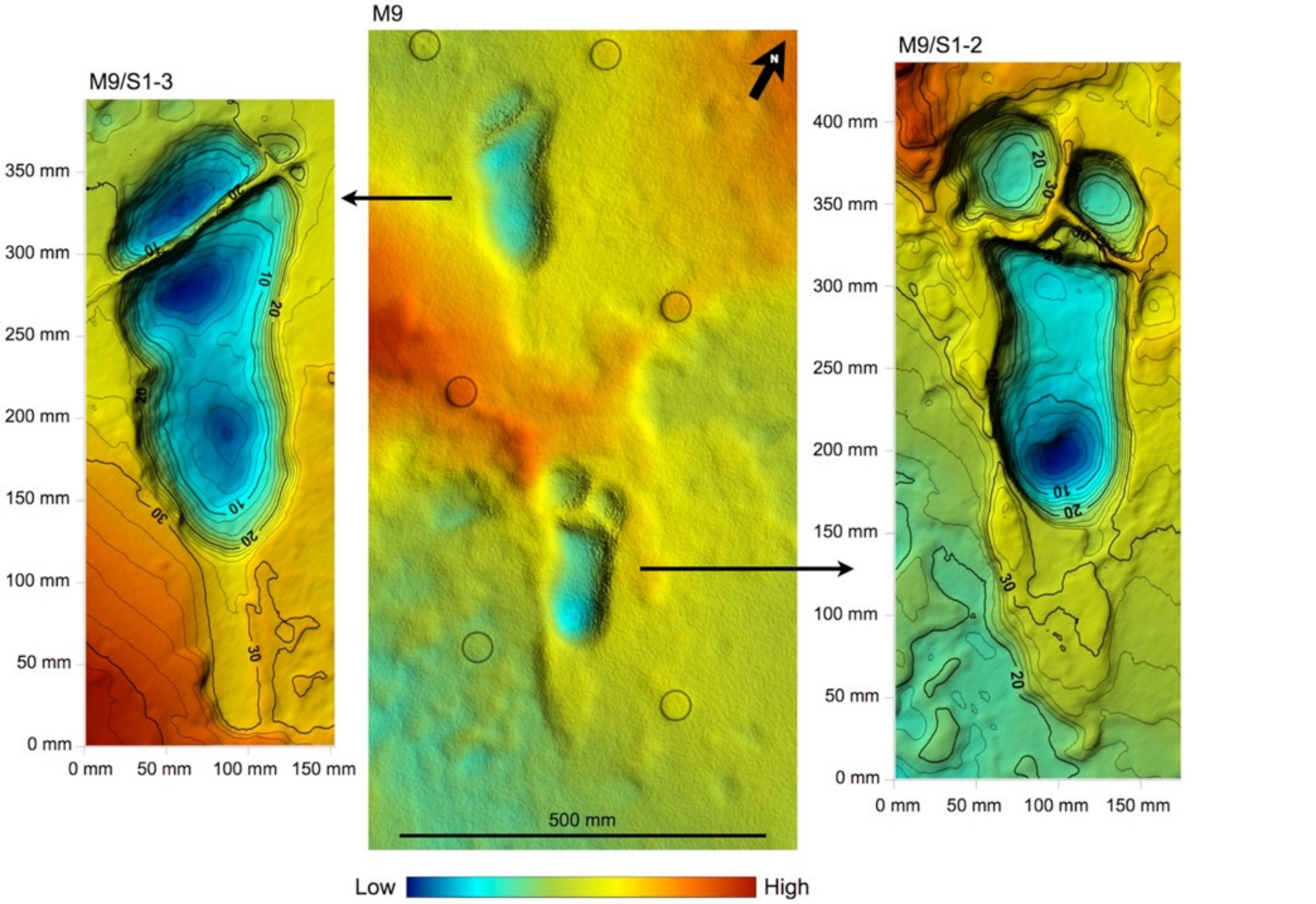

Figure 5. Shaded 3D photogrammetric elevation model of the central portion of test-pit M9 and close-up of the best-preserved tracks with contour lines. Colour renders heights as in the colour bar; distance between elevation contour lines is 2 mm. The empty circles indicate the position of the targets.

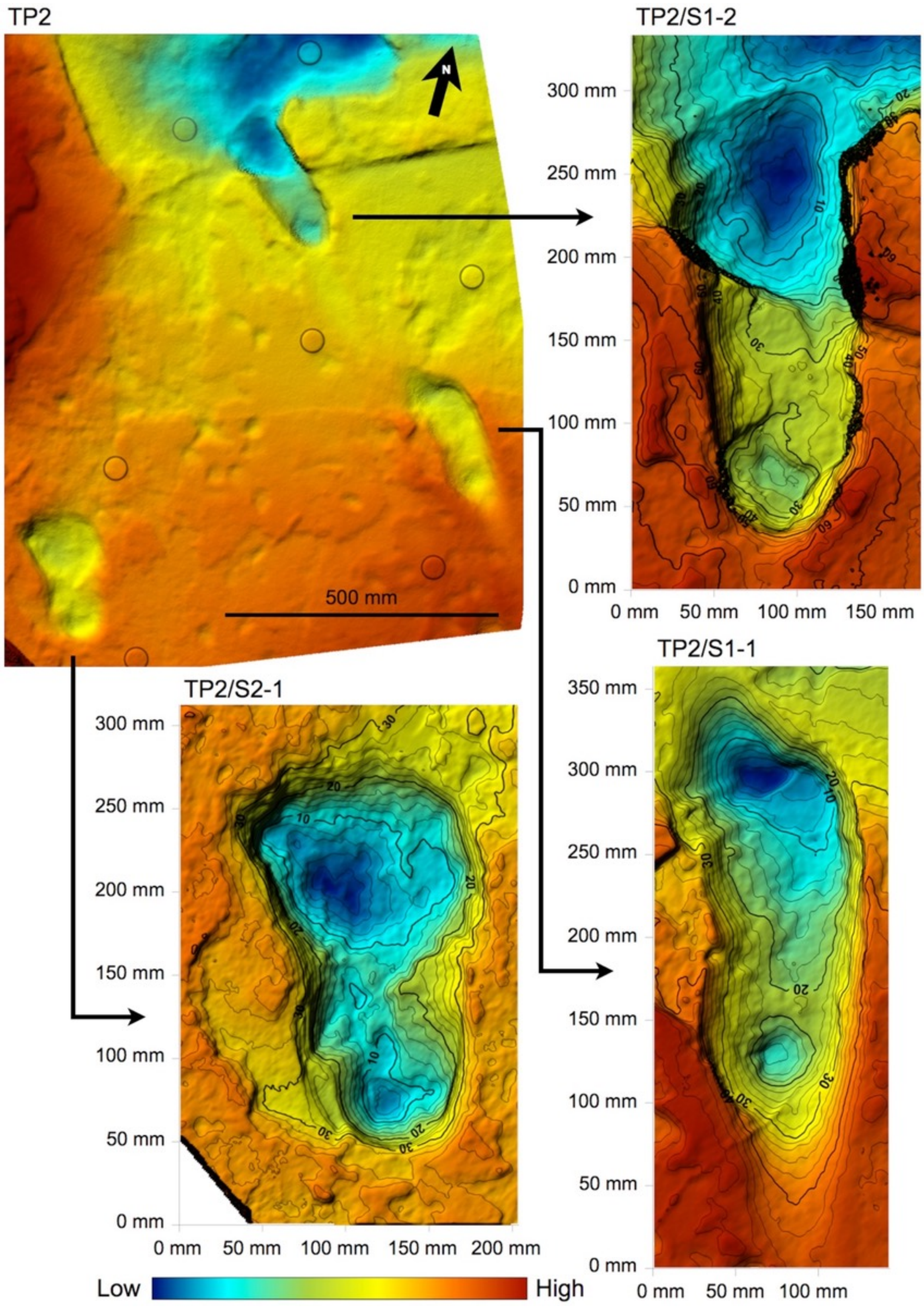

Figure 6. Shaded 3D photogrammetric elevation model of test-pit TP2 and close-up of the three hominin tracks with contour lines. Colour renders heights as in the colour bar; distance between elevation contour lines is 2 mm. The empty circles indicate the position of the targets.

Figure 7. Southern part of the hominin trackway in test-pit L8. Footprints L8/S1-1, L8/S1-2, L8/S1-3 and L8/S1-4 are visible from left to right. The heel drag mark is well visible posteriorly to L8/S1-3.

Figure 8. Test-pit L8 at Laetoli Site S. In the northern part of the test-pit (at the top), the Footprint Tuff is particularly altered, damaged by plant roots and dislodged along natural fractures.

Figure 9. Central part of the hominin trackway in the test-pit M9. Tracks M9/S1-3 and M9/S1-2 are visible from left to right. The two tracks are crossed by some fractures filled by hard calcite veins, which were not removed. In M9, the Footprint Tuff is in almost pristine conditions, and most of the tracks are still filled by compact sediment.

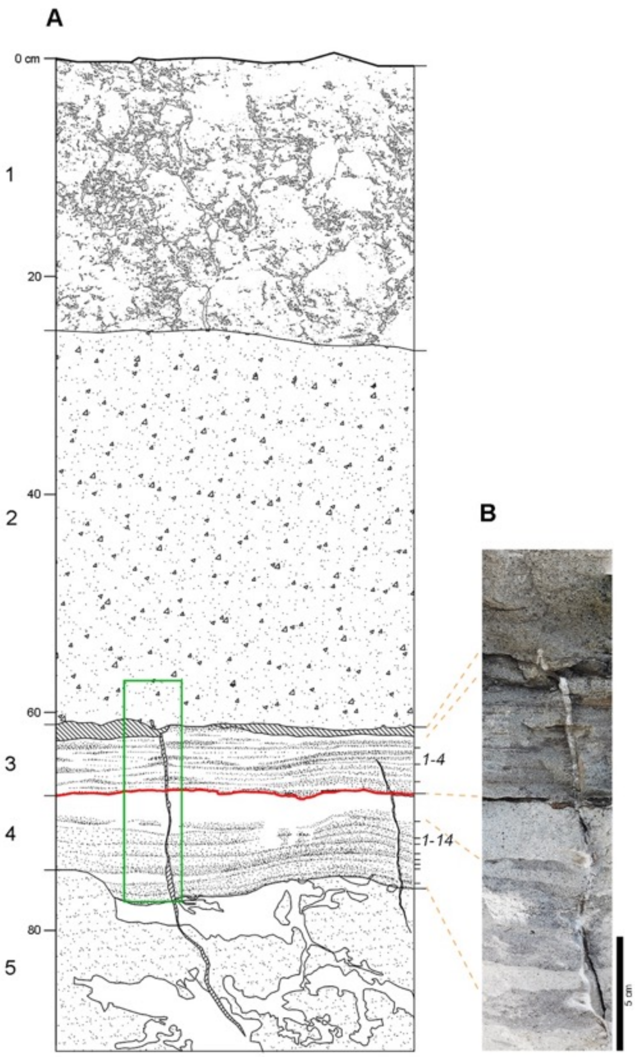

Figure 10. Laetoli Site S geology. (**A**) Stratigraphic sketch of the sequence, as in test-pit M9. Numbers on the left (1–5) correspond to the lithologic units observed in the field; 1: modern soil; 2: grey augite-rich tuff; 3: laminated grey tuff; 4: finely layered grey and white tuff; 5: light brown tuff. Unit 2 corresponds to the Augite Biotite Tuff (***Hay, 1987***); units 3 and 4 correspond respectively to the upper and lower horizons of the Footprint Tuff (***Hay, 1987***). Numbers on the right indicate the four and fourteen sublevels included respectively in the upper and lower part (***Hay, 1987***). Hominin tracks occur on the topmost sublevel of unit 4 (red line); a similar thick whitish footprint-bearing level can be observed in the same stratigraphic position at Localities 6 and 7. Oblique hatch: open cracks. White patches in 5 are burrower tunnels and disturbances. Green rectangle: location of panel B image. (**B**) Photomosaic showing the Footprint Tuff and part of the overlying unit.

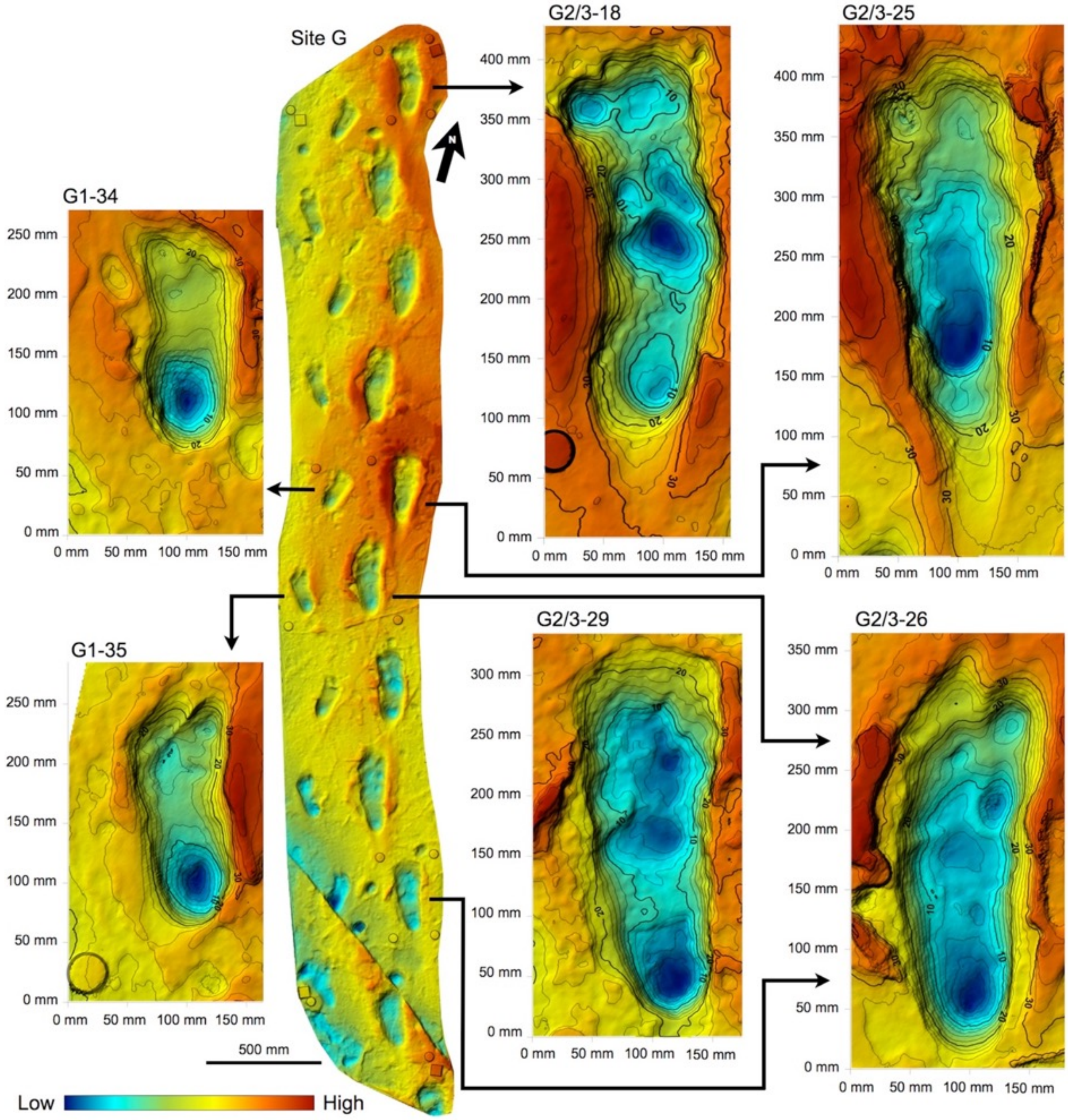

Figure 11. Shaded 3D photogrammetric model of a cast of the southern portion of the Site G trackway with close-up of selected hominin tracks with contour lines. Colour is rendered with 10-mm isopleths for the trackway and 2-mm isopleths for the single tracks. The empty circles and squares indicate the position of the targets.

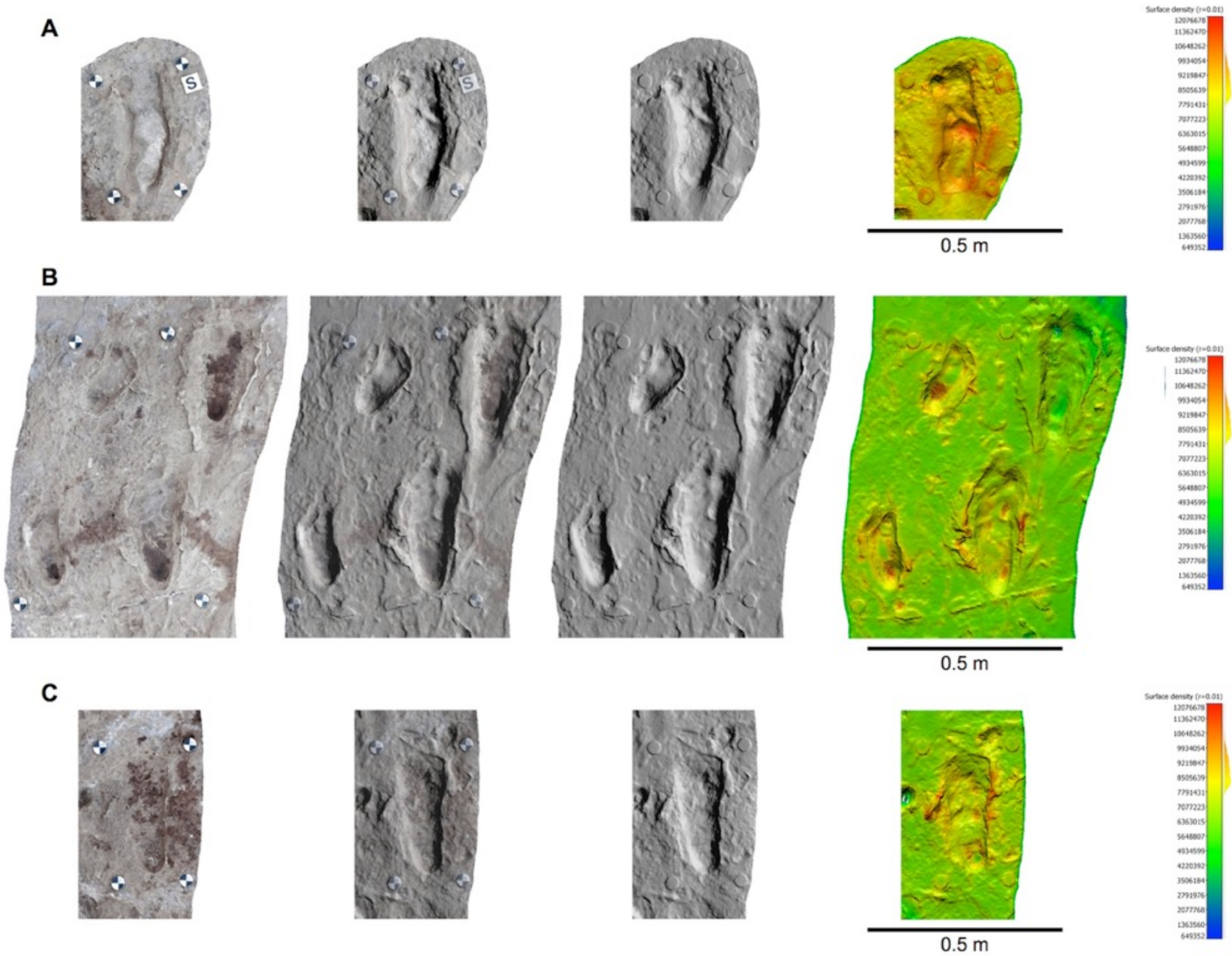

Figure 11—figure supplement 1. Orthophotos of selected hominin footprints from a cast of the southern portion of the Site G trackway. (**A**) G2/3-29. (**B**) G1-34, G1-35, G2/3-25, G2/3-26. (**C**) G2/3-18. From left to right: textured models, textured and shaded models, shaded models, and shaded coloured models. Colours represent the density of the point clouds by determining the distance to the nearest neighbour. The surface density is the calculation of number of neighbours divided by the neighbourhood surface = $N/(\pi R^2)$.

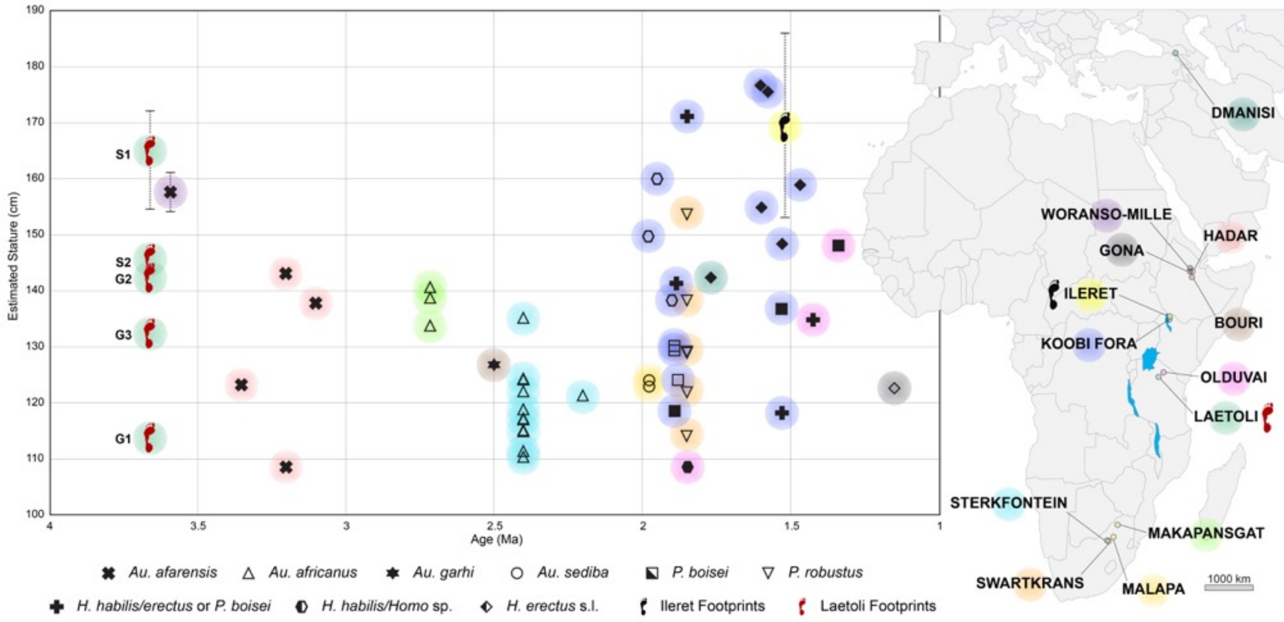

Figure 12. Estimates of predicted stature for fossil hominin individuals by species over time for the interval 4–1 Ma. Solid symbols (or crosses in bold) refer to stature estimates based on actual femur length; open symbols refer to stature estimates based on estimated femur length, in turn based on femur head diameter. For Laetoli and Ileret, stature estimates are based on footprint length (see Materials and Methods). For Laetoli, Ileret and Woranso-Mille the average value and range of predicted stature are shown. Colours are associated to the geographical location of each fossil/footprint sites on the map. See ***Supplementary file 5*** for details.

Table 1. Number of individual tracks (excluding hominins) at Laetoli Site S.

Taxon	L8	M9	TP2	M10	Total
Numididae (?*Numida*)	-	4	-	9	13
Bovidae, small size (?*Madoqua*)	107	39	16	211	373
Bovidae, medium size (?*Gazella*)	39	9	-	21	79
Equidae (?*Hipparion*)	1	2	-	-	3
Giraffidae	-	-	-	4	4
Lagomorpha (?*Lepus*)	8	-	-	4	12
Rhinocerotidae	-	1	-	-	1
Unidentified micromammals	-	27	-	17	44
Total	155	82	26	266	529

Table 2. Dimensional parameters measured and derived from the Laetoli Site S tracks and stature and body mass estimates for S1 and S2.

Footprint	Side	Length (mm)	Max width (mm)	Foot index (%)	Heel width (mm)	Angle of gait (degrees)	Estimated stature (cm)			Estimated body mass (kg)	
							H. sapiens[§]	*H. sapiens*[°]	*A. afarensis*[‡]	*H. sapiens*[°]	*A. afarensis*[‡]
TP2/S1-1	right	271	101	37.2	83	6	194–170	175.4	167–175	53.8	42.9–50.0
TP2/S1-2	left	271	99	36.6	81	4	193–169	175.1	167–175	53.1	42.8–49.8
M9/S1-1	left	250	102	40.6	73	2	179–156	167.5	154–161	51.6	39.6–46.0
M9/S1-2	right	264	105	39.7	80	3	189–165	172.8	163–171	54.2	41.8–48.7
M9/S1-3	left	268	111	41.2	91	4	192–168	174.3	166–173	56.3	42.5–49.4
M9/S1-4	right	245	101	41.2	71	4	175–153	165.6	151–158	50.9	38.8–45.1
L8/S1-1	right	245	104	42.4	78	8	175–153	165.6	151–158	51.7	38.8–45.1
L8/S1-2	left	265	106	40.0	82	11	189–166	173.1	164–171	54.5	41.9–48.8
L8/S1-3	right	260	103	39.6	77	3	186–163	171.3	161–168	53.1	41.2–47.9
L8/S1-4	left	274	106	38.6	81	10	196–171	176.5	169–177	55.6	43.4–50.5
L8/S1-5	right	-	-	-	-	-	-	-	-	-	-
L8/S1-6	left	-	-	-	86	3	-	-	-	-	-
L8/S1-7	right	258	110	42.7	90	8	184–161	170.3	159–166	54.8	40.7–47.4
Average S1	**-**	**261**	**104**	**40.0**	**81**	**6**	**184–163**	**171.6**	**161–168**	**53.6**	**41.3–48.1**
TP2/S2-1	right	231	120*	51.9*	86	-	165–144	160	142–149	46.7	36.5–42.4

Step length

Footprints	Side	Step length (mm)
TP2/S1-1 ⇢ 2	right ⇢ left	553
M9/S1-1 ⇢ 2	left ⇢ right	548
M9/S1-2 ⇢ 3	right ⇢ left	505
M9/S1-3 ⇢ 4	left ⇢ right	571
L8/S1-1 ⇢ 2	right ⇢ left	552
L8/S1-2 ⇢ 3	left ⇢ right	587
L8/S1-3 ⇢ 4	right ⇢ left	573
L8/S1-6 ⇢ 7	left ⇢ right	660
Average right ⇢ left		545
Average left ⇢ right		591
Average		568

Stride length

Footprints	Side	Stride length (mm)
M9/S1-1 ⇢ 3	left	1044
M9/S1-2 ⇢ 4	right	1069
L8/S1-1 ⇢ 3	right	1140
L8/S1-2 ⇢ 4	left	1159
L8/S1-4 ⇢ 6	left	1284
Average right		1105
Average left		1162
Average		1139

*Values overestimated because of the enlarged morphology of the only preserved track of S2. §Estimation based on the relationship between foot length and stature in *H. sapiens* (***Tuttle, 1987***). °Estimation based on the relationship between footprint length and stature/body mass in *H. sapiens* (***Dingwall et al., 2013***). ‡Estimation based on the relationship between foot length and stature/body mass in *A. afarensis* (***Dingwall et al., 2013***). See Materials and Methods for details.

Table 3. Average data and estimates for the five Laetoli track-makers from Sites S and G

Trackway		**S1**	**S2**	**G1**	**G2**	**G3**
Number of measurable footprints		11	1	9	2	8
Average footprint length (mm)		261	231	180	225	209
Average footprint max width (mm)		104	120[*]	79	117	85
Average foot index (%)		40.0	51.9[*]	43.8	48.0	41.5
Average step length (mm)		568	-	416	453	433
Average stride length (mm)		1139	-	829	880	876
Estimated stature (cm)	*H. sapiens*[§]	163–186	144–165	113–129	141–161	130–149
	H. sapiens[°]	171.6 ± 5.4	160 ± 5.4	141.4 ± 5.4	158.2 ± 5.4	152.2 ± 5.4
	A. afarensis[‡]	161–168	142–149	111–116	139–145	129–135
Estimated body mass (kg)	*H. sapiens*[°]	53.6 ± 3.7	46.7 ± 3.8	39.3 ± 3.7	52.6 ± 3.7	43.2 ± 3.7
	A. afarensis[‡]	41.3–48.1	36.5–42.4	28.5–33.1	35.6–41.4	33.1–38.5
Walking speed (m/s)		0.47–0.55 (0.93)	-	0.43–0.50 (1.00)	0.36–0.42 (0.79)	0.39–0.46 (0.88)
Relative speed (s^{-1})		0.25–0.34 (0.54)	-	0.33–0.44 (0.71)	0.23–0.30 (0.50)	0.26–0.35 (0.58)

*Values overestimated because of the enlarged morphology of the only preserved track of S2. §As in Table 2. °As in Table 2. ‡ As in Table 2. For walking speed and relative speed, values outside the brackets are based on the method of ***Alexander (1976)***, those inside the brackets are based on the method of ***Dingwall et al. (2013)***. See Materials and Methods for details.

Supplementary file 1. Footprint imaging, measurement report 1.

Fieldwork measurement acquisition and error calculation.

ID TRENCH	ID MEASURE	ID 1° TARGET	H 1° TARGET (m)	ID 2° TARGET	H 2° TARGET (m)	DISTANCE (m)	Δ MEASURED (m)	Δ CORRECTED (m)	
L8	1	A	0.775	B	0.725	2.561	0.050	0.051	
L8	2	B	0.774	C	0.921	3.271	-0.147	-0.146	
L8	3	C	0.486	D	0.613	3.441	-0.127	-0.126	
L8	4	D	0.702	A	0.482	3.591	0.220	0.221	
L8	5	A	0.523	C	0.620	4.176	ERROR (m)	ERROR DISTRIBUT. (m)	FINAL ERROR (m)
L8	6	B	0.453	D	0.724	4.894	-0.004	-0.001	0.000
M9	7	E	0.660	F	0.622	2.335	0.038	0.038	
M9	8	F	0.705	G	0.690	2.861	0.015	0.015	
M9	9	G	0.736	H	0.720	2.884	0.016	0.016	
M9	10	H	0.799	E	0.867	3.951	-0.068	-0.068	
M9	11	E	0.745	G	0.690	4.276	ERROR (m)	ERROR DISTRIBUT. (m)	FINAL ERROR (m)
M9	12	F	0.808	H	0.765	4.209	0.001	0.000	0.000
TP2	13	I	0.581	J	0.600	1.333	-0.019	-0.020	
TP2	14	J	0.587	K	0.548	1.581	0.039	0.039	
TP2	15	K	0.549	L	0.518	1.444	0.031	0.031	
TP2	16	L	0.477	I	0.526	1.831	-0.049	-0.050	
TP2	17	I	0.517	K	0.498	2.231	ERROR (m)	ERROR DISTRIBUT. (m)	FINAL ERROR (m)
TP2	18	J	0.544	L	0.469	2.169	0.002	0.000	0.000
M10	19	M	0.701	N	0.686	2.211	0.015	0.015	
M10	20	N	0.658	O	0.578	3.696	0.080	0.081	
M10	21	O	0.609	P	0.614	2.304	-0.005	-0.004	
M10	22	P	0.566	M	0.658	3.621	-0.092	-0.092	
M10	23	M	0.659	O	0.562	4.291	ERROR (m)	ERROR DISTRIBUT. (m)	FINAL ERROR (m)
M10	24	N	0.645	P	0.564	4.306	-0.002	-0.001	0.000

Supplementary file 2. Footprint imaging, measurement report 2.

STAR*NET reports of measurements in plan and altitude and calculation of the new adjusted x,y,z-coordinates.

STAR*NET REPORT OF L8 (PLAN)						
Adjustment Statistical Summary						
Iterations		2				
Number of Stations		4				
Number of Observations		11				
Number of Unknowns		5				
Number of Redundant Obs		6				
Adjusted Station Information						
Adjusted Coordinates (Meters)						
Station	**E**	**N**				
A	0.8470	0.0000				
B	3.4125	0.0000				
C	3.4331	3.2739				
D	-0.0041	3.4941				
Adjusted Observations and Residuals						
Adjusted Coordinate Observations (Meters) (Stations with Partially Fixed Coordinate Components)						
Station	**Component**	**Adj Coordinate**	**Residual**	**StdErr**	**StdRes**	**File:Line**
C	E	3.4331	-0.0099	0.0300	0.3	1:3
	N	3.2739	0.0029	0.0300	0.1	
D	E	-0.0041	-0.0041	0.0300	0.1	1:4
	N	3.4941	-0.0029	0.0300	0.1	
B	E	3.4125	0.0045	0.0300	0.2	1:2
Adjusted Distance Observations (Meters)						
From	**To**	**Distance**	**Residual**	**StdErr**	**StdRes**	**File:Line**
B	D	4.8869	-0.0071	0.0091	0.8	1:16
D	A	3.5963	0.0053	0.0091	0.6	1:13
A	B	2.5655	0.0045	0.0091	0.5	1:7
A	C	4.1721	-0.0039	0.0091	0.4	1:15
C	D	3.4443	0.0033	0.0091	0.4	1:11
B	C	3.274	0.003	0.0091	0.3	1:9

STAR*NET REPORT OF L8 (ALTITUDE)						
Adjustment Statistical Summary						
Number of Stations		4				
Number of Observations		6				
Number of Unknowns		3				
Number of Redundant Obs		3				
Adjusted Station Information						
Adjusted Elevations and Error Propagation (Meters)						
Station	**Elev**	**StdDev**	**95**			
A	1.0000	0.0000	0.0000			
B	1.0503	0.0010	0.0019			
C	0.9040	0.0010	0.0020			
D	0.7787	0.0010	0.0021			
Adjusted Observations and Residuals						
Adjusted Differential Level Observations (Meters)						
From	**To**	**Elev Diff**	**Residual**	**StdErr**	**StdRes**	**File:Line**
C	D	-0.1253	0.0017	0.0003	5.6*	1:8
D	A	0.2213	0.0013	0.0003	4.3*	1:9
A	C	-0.0960	0.0010	0.0003	3.2*	1:10
B	C	-0.1462	0.0008	0.0003	2.6	1:7
B	D	-0.2716	-0.2716	0.0003	1.7	1:11
A	B	0.0503	0.0503	0.0003	1.1	1:6

STAR*NET REPORT OF M9 (PLAN)

Adjustment Statistical Summary

Iterations	2
Number of Stations	4
Number of Observations	11
Number of Unknowns	5
Number of Redundant Obs	6

Adjusted Station Information

Adjusted Coordinates (Meters)

Station	E	N
E	0.0000	0.0000
F	2.3344	0.0000
G	3.3322	2.6807
H	0.7124	3.8853

Adjusted Observations and Residuals

Adjusted Coordinate Observations (Meters) (Stations with Partially Fixed Coordinate Components)

Station	Component	Adj Coordinate	Residual	StdErr	StdRes	File:Line
G	E	3.3322	0.0022	0.0300	0.1	1:3
	N	2.6807	-0.0013	0.0300	0.0	
H	E	0.7124	0.0014	0.0300	0.0	1:4
	N	3.8853	0.0003	0.0300	0.0	
F	E	2.3344	-0.0006	0.0300	0.0	1:2

Adjusted Distance Observations (Meters)

From	To	Distance	Residual	StdErr	StdRes	File:Line
F	H	4.2102	0.0012	0.0091	0.1	1:11
H	E	3.9500	-0.0010	0.0091	0.1	1:9
E	G	4.2767	0.0007	0.0091	0.1	1:10
E	F	2.3344	-0.0006	0.0091	0.1	1:6
F	G	2.8604	-0.0006	0.0091	0.1	1:7
G	H	2.8834	-0.0006	0.0091	0.1	1:8

STAR*NET REPORT OF M9 (ALTITUDE)

Adjustment Statistical Summary

Number of Stations	4
Number of Observations	6
Number of Unknowns	3
Number of Redundant Obs	3

Adjusted Station Information

Adjusted Elevations and Error Propagation (Meters)

Station	Elev	StdDev	95
E	1.000000	0.000002	0.000003
F	1.036200	0.003261	0.006392
G	1.053900	0.003580	0.007018
H	1.072000	0.003644	0.007142

Adjusted Observations and Residuals

Adjusted Differential Level Observations (Meters)

From	To	Elev Diff	Residual	StdErr	StdRes	File:Line
F	H	0.0358	-0.0072	0.0003	22.3*	1:11
H	E	-0.0720	-0.0040	0.0003	12.7*	1:9
F	G	0.0177	0.0027	0.0003	10.2*	1:7
G	H	0.0180	0.0020	0.0003	7.6*	1:8
E	F	0.0362	-0.0018	0.0003	7.4*	1:6
E	G	0.0539	-0.0011	0.0003	3.2*	1:10

STAR*NET REPORT OF TP2 (PLAN)						
Adjustment Statistical Summary						
Iterations		2				
Number of Stations		4				
Number of Observations		11				
Number of Unknowns		5				
Number of Redundant Obs		6				
Adjusted Station Information						
Adjusted Coordinates (Meters)						
Station	**E**	**N**				
I	0.0000	0.0000				
J	1.3348	0.0000				
K	1.5908	1.5616				
L	0.1694	1.8256				
Adjusted Observations and Residuals						
Adjusted Coordinate Observations (Meters) (Stations with Partially Fixed Coordinate Components)						
Station	**Component**	**Adj Coordinate**	**Residual**	**StdErr**	**StdRes**	**File:Line**
K	E	1.5908	-0.0052	0.0300	0.2	1:3
	N	1.5616	0.0026	0.0300	0.1	
L	E	0.1694	-0.0036	0.0300	0.1	1:4
	N	1.8256	-0.0004	0.0300	0.0	
J	E	1.3348	0.0018	0.0300	0.1	1:2
Adjusted Distance Observations (Meters)						
From	**To**	**Distance**	**Residual**	**StdErr**	**StdRes**	**File:Line**
J	L	2.1658	-0.0032	0.0091	0.3	1:11
L	I	1.8334	0.0024	0.0091	0.3	1:9
I	K	2.2291	-0.0019	0.0091	0.2	1:10
I	J	1.3348	0.0018	0.0091	0.2	1:6
K	L	1.4456	0.0016	0.0091	0.2	1:8
J	K	1.5824	0.0014	0.0091	0.2	1:7

STAR*NET REPORT OF TP2 (ALTITUDE)						
Adjustment Statistical Summary						
Number of Stations		4				
Number of Observations		6				
Number of Unknowns		3				
Number of Redundant Obs		3				
Adjusted Station Information						
Adjusted Elevations and Error Propagation (Meters)						
Station	**Elev**	**StdDev**	**95**			
I	1.000000	0.000001	0.000002			
J	0.979500	0.001645	0.003224			
K	1.019200	0.001766	0.003461			
L	1.051000	0.001750	0.003431			
Adjusted Observations and Residuals						
Adjusted Differential Level Observations (Meters)						
From	**To**	**Elev Diff**	**Residual**	**StdErr**	**StdRes**	**File:Line**
J	L	0.0715	-0.0035	0.0002	15.0*	1:11
L	I	-0.0510	-0.0020	0.0002	9.2*	1:9
I	J	-0.0205	-0.0015	0.0002	8.4*	1:6
K	L	0.0318	0.0008	0.0002	4.1*	1:8
J	K	0.0397	0.0007	0.0002	3.6*	1:7
I	K	0.0192	0.0002	0.0002	0.8	1:10

STAR*NET REPORT OF M10 (PLAN)

Adjustment Statistical Summary

Iterations	1
Number of Stations	4
Number of Observations	11
Number of Unknowns	5
Number of Redundant Obs	6

Adjusted Station Information

Adjusted Coordinates (Meters)

Station	E	N
M	0.1220	0.0000
N	2.3330	0.0000
O	2.3025	3.6958
P	-0.0003	3.6190

Adjusted Observations and Residuals

Adjusted Coordinate Observations (Meters) (Stations with Partially Fixed Coordinate Components)

Station	Component	Adj Coordinate	Residual	StdErr	StdRes	File:Line
O	E	2.3025	-0.0005	0.0300	0.0	1:3
	N	3.6958	-0.0002	0.0300	0.0	
P	E	-0.0003	-0.0003	0.0300	0.0	1:4
	N	3.6190	0.0000	0.0300	0.0	
N	E	2.3330	0.0000	0.0300	0.0	1:2

Adjusted Distance Observations (Meters)

From	To	Distance	Residual	StdErr	StdRes	File:Line
M	O	4.2911	0.0001	0.0091	0.0	1:10
N	O	3.6959	-0.0001	0.0091	0.0	1:7
N	P	4.3059	-0.0001	0.0091	0.0	1:11
P	M	3.6210	0.0000	0.0091	0.0	1:9
M	N	2.2110	0.0000	0.0091	0.0	1:6
O	P	2.3040	0.0000	0.0091	0.0	1:8

STAR*NET REPORT OF M10 (ALTITUDE)

Adjustment Statistical Summary

Number of Stations	4
Number of Observations	6
Number of Unknowns	3
Number of Redundant Obs	3

Adjusted Station Information

Adjusted Elevations and Error Propagation (Meters)

Station	Elev	StdDev	95
M	1.000000	0.000001	0.000001
N	1.014700	0.001340	0.002627
O	1.096700	0.001479	0.002898
P	1.092800	0.001458	0.002857

Adjusted Observations and Residuals

Adjusted Differential Level Observations (Meters)

From	To	Elev Diff	Residual	StdErr	StdRes	File:Line
N	P	0.0781	-0.0029	0.0003	8.9*	1:11
N	O	0.0820	0.0020	0.0003	6.6*	1:7
O	P	-0.0039	0.0011	0.0003	4.5*	1:8
P	M	-0.0928	-0.0008	0.0003	2.5	1:9
M	O	0.0967	-0.0003	0.0003	0.9	1:10
M	N	0.0147	-0.0003	0.0003	1.3	1:6

Supplementary file 3. Footprint imaging, measurement report 3.

Adjusted x,y,z-coordinate set of the control points.

ID POINT	X	Y	Z
A	0.847	0.000	1.000
B	3.412	0.000	1.050
C	3.433	3.274	0.904
D	-0.004	3.494	0.779
E	0.000	0.000	1.000
F	2.334	0.000	1.036
G	3.332	2.681	1.054
H	0.712	3.885	1.072
I	0.000	0.000	1.000
J	1.335	0.000	0.979
K	1.591	1.562	1.019
L	0.170	1.826	1.051
M	0.122	0.000	1.000
N	2.333	0.000	1.015
O	2.303	3.696	1.097
P	0.000	3.619	1.093

Supplementary file 4. Footprint imaging, measurement report 4.

Photoscan reports of photogrammetric processing.

ID DATA	PICTURES (n°)	TIE POINTS (n° points)	DENSE CLOUD (n° points)	MESH (n° faces)	TEXTURE (pixel)
L8	171	15,755	6,523,219	6,000,000	6,000 x 6,000
L8/S1-1	31	4,885	12,788,392	1,000,000	4,096 x 4,096
L8/S1-2	31	5,105	11,956,726	1,000,000	4,096 x 4,096
L8/S1-3	34	6,721	14,577,445	1,000,000	4,096 x 4,096
L8/S1-4	38	5,754	13,849,615	1,000,000	4,096 x 4,096
M9	277	16,752	5,520,206	5,000,000	6,000 x 6,000
M9/S1-2	97	7,095	3,044,911	1,000,000	4,096 x 4,096
M9/S1-3	90	6,695	3,024,744	1,000,000	4,096 x 4,096
TP2	180	14,476	4,803,978	4,000,000	6,000 x 6,000
TP2/S2-1	89	6,326	9,388,424	1,000,000	4,096 x 4,096
TP2/S1-1	55	4,434	3,624,823	1,000,000	4,096 x 4,096
TP2/S1-2	56	3,991	4,127,016	1,000,000	4,096 x 4,096
M10	127	11,254	4,969,463	5,000,000	6,000 x 6,000
M10/AF1	33	3,704	1,879,530	1,000,000	4,096 x 4,096
M10/AF2	34	3,512	2,204,826	1,000,000	4,096 x 4,096
M10/AF3	42	4,322	3,306,688	1,000,000	4,096 x 4,096
Site G trackway	117	3,871	2,968,040	3,000,000	6,000 x 6,000
G2/3-18	30	6,627	1,584,588	1,000,000	4,096 x 4,096
G1-34-35, G2/3-25-26	69	12,607	4,962,963	2,000,000	4,096 x 4,096
G2/3-29	35	8,239	1,677,459	1,000,000	4,096 x 4,096

Supplementary file 5. Individual fossil ages, localities and estimated statures used to build ***Figure 12***.

All ages are from ***Grabowski et al. (2015)***, unless otherwise stated. Actual femur lengths include both measurements of complete femora and length estimations based on reconstruction of incomplete bones. Actual femur lengths are from ***McHenry (1991)***, unless otherwise indicated. When the actual femur length was not available, it was estimated from the femur head diameter (FHD) (***McHenry, 1991***). Stature estimates in red were used to build ***Figure 12***. Femur measurements are in mm, statures are in cm.

Specimen	Taxon	Locality	Age	Actual Femur Length	FHD	Estimated Femur Length	Stature McHenry (1991)	Stature Jungers et al. (2016)	Stature McHenry (1991)	Stature Jungers et al. (2016)	Notes
							Using actual femur length		Using estimated femur length		
KNM-ER 1503	***P. boisei*?**	Koobi Fora	1,890	-	34,5	343	-	-	128	**129**	
KNM-ER 1505	***P. boisei*?**	Koobi Fora	1,890	-	34,7	345	-	-	129	**130**	
KNM-ER 738	***P. boisei*?**	Koobi Fora	1,880	-	33,0	327	-	-	122	**124**	
KNM-ER 1500d	***P. boisei*?**	Koobi Fora	1,890	310	-	-	116	**118**	-	-	Femur length estimated by McHenry (1991) on the basis of bone reconstruction.
KNM-ER 993	***P. boisei*?**	Koobi Fora	1,530	365	-	-	137	**137**	-	-	*P. boisei* in McHenry (1991). Femur length estimated by McHenry (1991) on the basis of bone reconstruction.
OH 80	***P. boisei***	Olduvai	1,338	400	-	-	150	**148**	-	-	Age and estimation of femur length are from Domínguez-Rodrigo et al. (2013).
SK 3155B	***P. robustus***	Swartkrans	1,850	-	32,4	320	-	-	120	**122**	
SK 50	***P. robustus***	Swartkrans	1,850	-	41,3	416	-	-	156	**154**	
SK 82	***P. robustus***	Swartkrans	1,850	-	34,5	343	-	-	128	**129**	
SK 97	***P. robustus***	Swartkrans	1,850	-	36,9	369	-	-	138	**138**	
SKW 19	***P. robustus***	Swartkrans	1,850	-	30,2	297	-	-	111	**114**	
SWT1/LB-2	***P. robustus***	Swartkrans	1,850	-	34,4	342	-	-	128	**129**	
KSD-VP-1/1	***Au. afarensis***	Woranso-Mille	3,590	*max* 438	-	-	164	**161**	-	-	Minimum and maximum estimations of femur length are from Haile-Selassie et al. (2010).
				mean 428	-	-	160	**158**	-	-	
				min 418	-	-	156	**154**	-	-	
A.L. 288-1	***Au. afarensis***	Hadar	3,200	280	-	-	105	**109**	-	-	
A.L. 827-1	***Au. afarensis***	Hadar	3,100	368	-	-	138	**138**	-	-	

A.L. 152-2	***Au. afarensis***	Hadar	3,350	324	33,1	328	121	**123**	123	124	Femur length estimated by Ward et al. (2012).
A.L. 333.3	***Au. afarensis***	Hadar	3,200	384	39,5	397	144	**143**	148	147	Femur length estimated by Ward et al. (2012).
Sts 14	***Au. africanus***	Sterkfontein	2,400	-	29,4	288	-	-	108	**111**	
Stw 25	***Au. africanus***	Sterkfontein	2,400	-	32,4	320	-	-	120	**122**	
Stw 392	***Au. africanus***	Sterkfontein	2,400	-	31,5	311	-	-	116	**119**	
Stw 361	***Au. africanus***	Sterkfontein	2,400	-	29,1	285	-	-	107	**110**	
Stw 403	***Au. africanus***	Sterkfontein	2,400	-	31,1	306	-	-	115	**117**	
Stw 431	***Au. africanus***	Sterkfontein	2,400	-	36,1	360	-	-	135	**135**	
Stw 479	***Au. africanus***	Sterkfontein	2,400	-	31,0	305	-	-	114	**117**	
Stw 501	***Au. africanus***	Sterkfontein	2,400	-	33,0	327	-	-	122	**124**	
Stw 31	***Au. africanus***	Sterkfontein	2,400	-	30,4	299	-	-	112	**115**	
Stw 522	***Au. africanus***	Sterkfontein	2,400	-	30,5	300	-	-	112	**115**	
Stw 527	***Au. africanus***	Sterkfontein	2,400	-	33,0	327	-	-	122	**124**	
Stw 598	***Au. africanus***	Sterkfontein	2,200	-	32,2	318	-	-	119	**121**	
MLD 17	***Au. africanus***	Makapansgat	2,715	-	37,6	376	-	-	141	**140**	
MLD 25	***Au. africanus***	Makapansgat	2,715	-	35,7	356	-	-	133	**134**	
MLD 46	***Au. africanus***	Makapansgat	2,715	-	37,1	371	-	-	139	**139**	
BOU-VP-12/1	***Au. garhi***	Bouri	2,500	335	-	-	125	**127**	-	-	Femur length is from Grabowski et al. (2015).
MH1	***Au. sediba*** **(juv)**	Malapa	1,977	-	33,0	327	-	-	122	**124**	
MH2	***Au. sediba***	Malapa	1,977	-	32,7	323	-	-	121	**123**	
OH 62	***H. habilis***	Olduvai	1,848	280	-	-	105	**109**	-	-	Femur length is from Grabowski et al. (2015).
KNM-ER 1472	***Homo*** **sp.**	Koobi Fora	1,980	-	40,2	404	-	-	151	**150**	*H. habilis* in McHenry (1991).
KNM-ER 1481	***Homo*** **sp.**	Koobi Fora	1,950	-	43,0	435	-	-	163	**160**	*H. habilis* in McHenry (1991).
KNM-ER 5881	***Homo*** **sp.**	Koobi Fora	1,900	-	37,0	370	-	-	138	**138**	
BSN49/P27	***H. erectus*** **s.l.**	Gona	1,150	-	32,6	322	-	-	121	**123**	
D 4167/3901	***H. erectus*** **s.l.**	Dmanisi	1,770	382	40,2	404	143	**142**	151	150	Femur length is from Grabowski et al. (2015).
KNM-ER 736	***H. erectus*** **s.l.**	Koobi Fora	1,580	482	-	-	180	**175**	-	-	*H. erectus*? in Grabowski et al. (2015). Age from Will and Stock (2015). Femur length estimated by McHenry (1991) on the basis of bone reconstruction.

KNM-ER 737	***H. erectus* s.l.?**	Koobi Fora	1,600	420	-	-	157	**155**	-	-	*H. erectus* in McHenry (1991). Femur length estimated by McHenry (1991) on the basis of bone reconstruction.
KNM-ER 803	***H. erectus* s.l.**	Koobi Fora	1,530	400	-	-	150	**148**	-	-	*H. erectus*? in Grabowski et al. (2015). Femur length estimated by McHenry (1991) on the basis of bone reconstruction.
KNM-ER 1808	***H. erectus* s.l.**	Koobi Fora	1,600	485	38,7	388	181	**176**	145	144	Age from Will and Stock (2015).
KNM-WT 15000	***H. erectus* s.l. (juv)**	Koobi Fora	1,470	432	45,9	466	162	**159**	174	170	Age from Will and Stock (2015).
KNM-ER 1463	***H. habilis/erectus* or *P. boisei***	Koobi Fora	1,530	310	-	-	116	**118**	-	-	*H. erectus/P. boisei* in McHenry (1991). Femur length estimated by McHenry (1991) on the basis of bone reconstruction.
OH 53	***H. habilis/erectus* or *P. boisei***	Olduvai	1,425	360	-	-	135	**135**	-	-	*H. habilis/P. boisei* in McHenry (1991). Femur length estimated by McHenry (1991) on the basis of bone reconstruction.
KNM-ER 1592	***H. habilis/erectus* or *P. boisei***	Koobi Fora	1,850	470	-	-	176	**171**	-	-	*H. habilis/P. boisei* in McHenry (1991). Femur length estimated by McHenry (1991) on the basis of bone reconstruction.
KNM-ER 3728	***H. habilis/erectus* or *P. boisei***	Koobi Fora	1,890	380	-	-	142	**142**	-	-	*H. habilis/P. boisei* in McHenry (1991); *P. boisei* in Wood (2013); Hominini indet. in Grabowsky et al. (2015); *H. habilis/H. rudolfensis/P. boisei* in Will and Stock (2015). Femur length estimated by McHenry (1991) on the basis of bone reconstruction.

FOOTPRINTS

Specimen	Taxon	Locality	Age	Estimated stature		Notes
-				*max*	186	
-	***H. erectus* s.l.?**	Ileret	1,520	*mean*	169	Age (range 1.53–1.51 Ma) and estimated statures are from Dingwall et al. (2013).
-				*min*	153	
				max	172	
S1				*mean*	165	
				min	155	
S2	***Au. afarensis*?**	Laetoli	3,660	146		
G1				114		
G2				142		
G3				132		

Supplementary references

Domínguez-RodrigoM, Pickering TR, Baquedano E, Mabulla A, Mark DF, Musiba C, Bunn HT, Uribelarrea D, Smith V, Diez-Martin F, Pérez-González A, Sánchez P, Santonja M, Barboni D, Gidna A, Ashley G, Yravedra J, Heaton JL, Arriaza MC. 2013. First Partial Skeleton of a 1.34-Million-Year-Old *Paranthropus boisei* from Bed II, Olduvai Gorge, Tanzania. *PLOS ONE* **8**:e80347. doi: 10.1371/journal.pone.0080347.

Will M, Stock JT. 2015. Spatial and temporal variation of body size among early Homo. *Journal of Human Evolution* **82**:15–33. doi: 10.1016/j.jhevol.2015.02.009.